Anonymous Referee #1

This manuscript reports the measurement of 13 SOA tracers from both biogenic and anthropogenic precursors in the particulate samples collected at Nam Co. The seasonal variations of isoprene SOA, monoterpene SOA and aromatic SOA tracers at Nam Co were interpreted by the temperature effect on the precursor emission and gas/particle partitioning. Source apportionment was carried by using the SOA-tracer method and the backward trajectory analysis. This is a well written paper and could be accepted by ACP if the following issues were addressed.

1. The temperature change could have two opposite effects on the SOA production. Decreasing temperature could reduce the precursor emission but enhance the gas to particle partitioning. The interpretations of the seasonal variation of SOA levels are quite confusing. It would be much better to develop a simple model to quantitatively or semi-quantitatively evaluate the temperature effect here and reveal which process (emission or partitioning) is dominant.

Reply: We appreciate the suggestion. In the revised manuscript, we used the two-product model to estimate the temperature effect on partitioning. SOA yield (Y) of precursors could be expressed using an empirical relationship based on gas-particle partitioning of two semi-volatile products (Odum et al., 1996):

$$Y = M_0 \sum_{i}^{2} \frac{\alpha_i K_i}{1 + M_0 K_i}$$

where M_0 (μg m^{-3}) is the total concentration of absorbing organic material; α_i is the mass stoichiometric coefficient of the product *i*; K_i (m^3 μg^{-1}) is the temperature-dependent partitioning coefficient of the semi-volatile compound *i*. Assuming a constant activity coefficient and mean molecular weight, partitioning coefficient, K_i (T) at a certain temperature (T) could be estimated (Sheehan and Bowman, 2001):

$$K_i(T) = K_i^* \frac{T}{T^*} \, exp\left[\frac{H_i}{R}\left(\frac{1}{T} - \frac{1}{T^*}\right)\right]$$

Where K_i^* is an experimentally determined partitioning coefficient at a reference temperature, T^*; H_i is the vaporization enthalpy; R is the gas constant. To model the temperature-dependent absorptive partitioning, three parameters, α_i, K_i, and H_i, are required for each condensable product.

Table 1 lists all the parameters for the two-product model of α-pinene SOA which were also used to estimate the temperature effect on SOA partitioning by Sheehan and Bowman (2001). The available data of OC at the NC site were reported in the range of 1.18 to 2.26 μgC m^{-3} during July 2006 to January 2007 with an average of 1.66 μgC m^{-3} (Ming et al., 2010). Thus, M_0 is calculated as 2.32 μg m^{-3} by the average OC multiplying 1.4.

Table 1 Two-product model parameters for α-pinene SOA

α_1	0.038
α_2	0.326
K_1^* (mg/μg)	0.171

K_2^* (mg/μg)	0.004
T* (K)	308
H_1=H_2 (kcal/mol)	17.5
R (J/K mol)	8.314

Monoterpene emission rate is solely dependent on temperature. The activity factor (γ_T) is expressed as (Guenther et al., 1993):

$$\gamma_T = exp^{\beta(T-T_s)}$$

Figure 1 shows the temperature dependence of α-pinene emission rate (γ_T) and SOA yield within the temperature range at the NC site. Obviously, decreasing temperature could reduce the precursor emission but enhance the gas to particle partitioning and SOA yield.

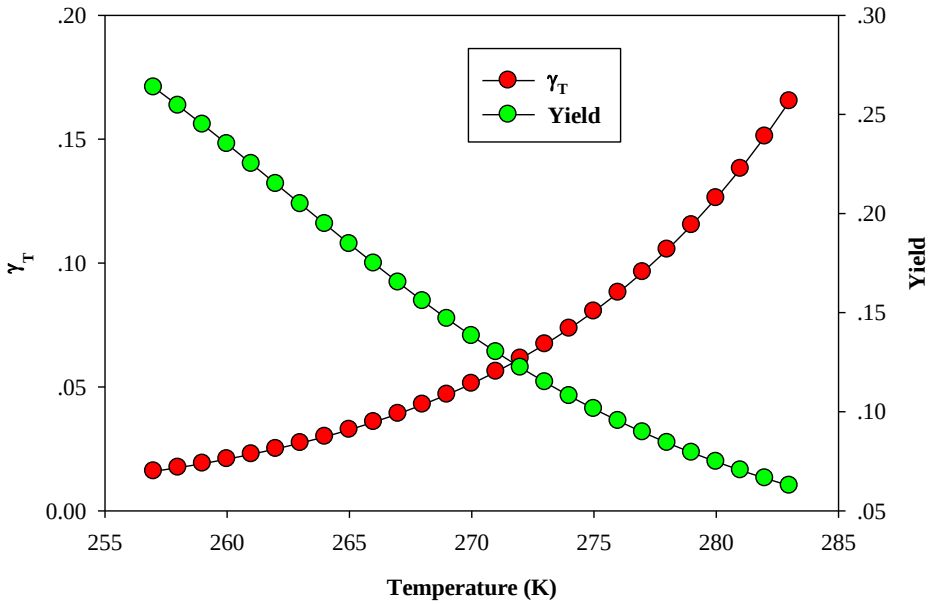

Figure 1 Temperature dependence of α-pinene emission rate (γ_T) and SOA yield

From July to November 2012 (period 1), high values of SOA_M tracers and SOA yield existed under low temperature, and SOA_M tracers were positively correlated with SOA yield ($r=0.647$, $p<0.05$, Figure 2a). These suggested that the temperature effect on partitioning was the dominant process influencing SOA variation during period 1. From December 2012 to April 2013 (period 2), high values of SOA_M tracers and activity factor (γ_T) existed under high temperature, and SOA_M tracers were positively correlated with γ_T ($r=0.741$, $p<0.05$, Figure 2b). These suggested that the temperature effect on emission was the dominant process influencing SOA variation during period 2. From May to July 2013 (period 3), SOA_M tracer concentrations were relative stable, and there was no correlation of SOA_M tracers with γ_T or SOA yield ($p>0.05$). These might result from the counteraction of temperature effects on emission and partitioning during the period 3.

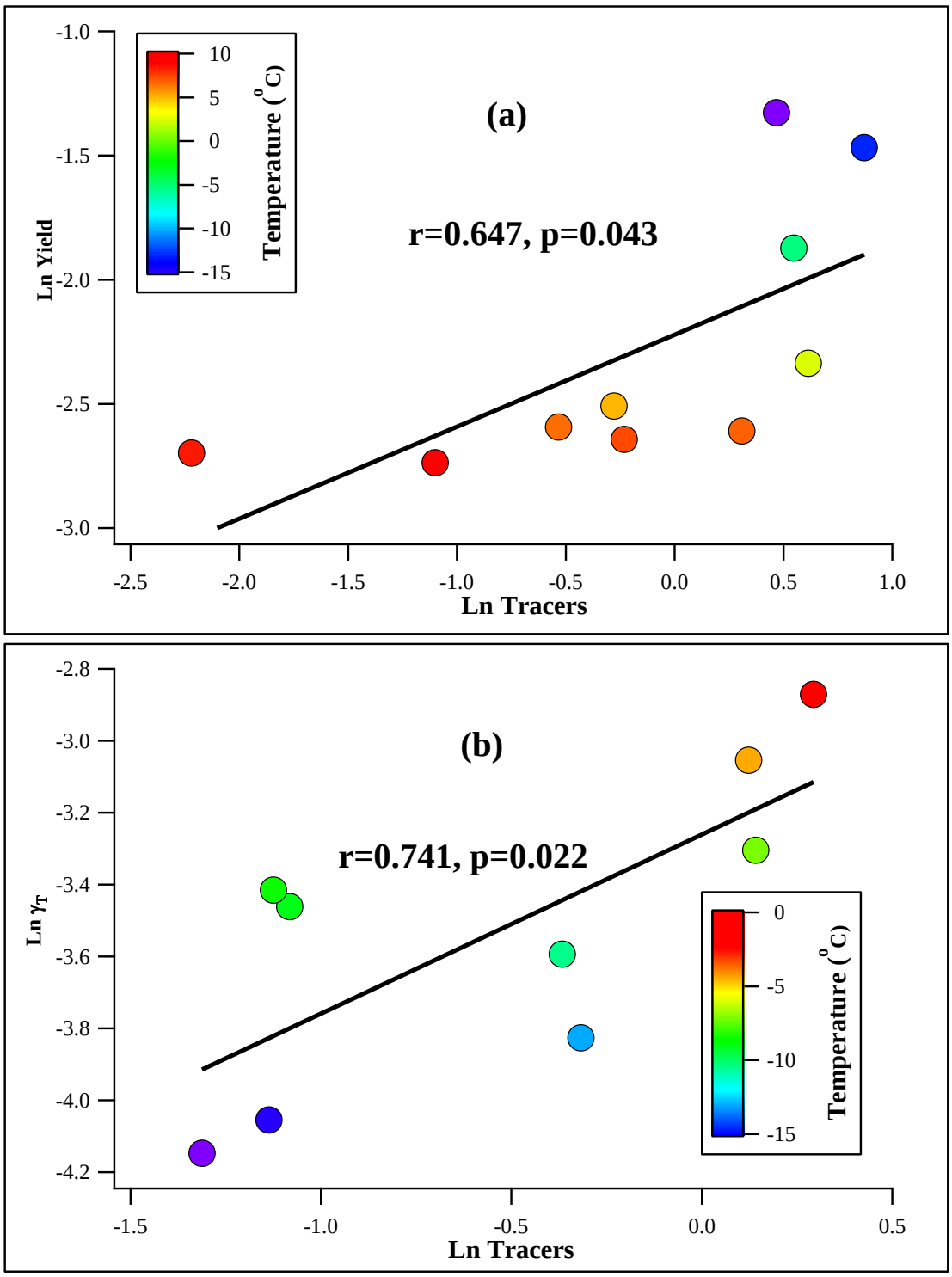

Figure 2 Correlation of monoterpene SOA tracers (SOA_M tracers) with SOA yield in period 1 (a) and γ_T in period 2 (b).

These interpretations of the seasonal variation of monoterpene SOA tracers were added in the revised manuscript (See below). Figure 2 was added in the revised manuscript as Figure 5. Figure 1 and Table 1 were added in the supplemental information file as Figure S5 and Table S2, respectively.

"SOA yield (Y) of precursors could be expressed using an empirical relationship

based on gas-particle partitioning of two semi-volatile products (Odum et al., 1996):

$$Y = M_0 \sum_i^2 \frac{\alpha_i K_i}{1+M_0 K_i} \quad (8)$$

where M_0 (μg m^{-3}) is the total concentration of absorbing organic material, α_i is the mass stoichiometric coefficients of the product i, K_i (m^3 μg^{-1}) is the temperature-dependent partitioning coefficient of the semi-volatile compound i. Assuming a constant activity coefficient and mean molecular weight, the partitioning coefficient, K_i (T) at a certain temperature (T) could be estimated as (Sheehan and Bowman, 2001):

$$K_i(T) = K_i^* \frac{T}{T^*} exp\left[\frac{H_i}{R}\left(\frac{1}{T} - \frac{1}{T^*}\right)\right] \quad (9)$$

where K_i^* is an experimentally determined partitioning coefficient at a reference temperature, T^*. H_i is the vaporization enthalpy, R is the gas constant. To model the temperature-dependent absorptive partitioning, three parameters, α_i, K_i, and H_i, are required for each condensable product.

Table S2 lists all the parameters for two-product model of α-pinene SOA which were also used to estimate the temperature effect on SOA partitioning by Sheehan and Bowman (2001). The available data of OC at the NC site were reported in the range of 1.18 to 2.26 μgC m^{-3} during July 2006 to January 2007 with an average of 1.66 μgC m^{-3} (Ming et al., 2010). Thus, M_0 is calculated as 2.32 μg m^{-3} by the average OC multiplying 1.4. Figure S5 shows the temperature dependence of α-pinene emission rate (γ_T) and SOA yield within the temperature range at the NC site (-16.7 to 10.2 ℃). Obviously, decreasing temperature could reduce the emission but enhance the gas to particle partitioning and SOA yield.

From July to November 2012 (period 1), high values of SOA_M tracers and SOA yield existed under low temperature, and SOA_M tracers were positively correlated with SOA yield (r=0.647, p<0.05, Figure 5a). These suggested that the temperature effect on partitioning was the dominant process influencing SOA_M tracers' variation during the period 1. From December 2012 to April 2013 (period 2), high values of SOA_M tracers and activity factor (γ_T) existed under high temperature, and SOA_M tracers were positively correlated with γ_T (r=0.741, p<0.05, Figure 2b). These suggested that the temperature effect on emission was the dominant process influencing SOA_M tracers' variation during the period 2. The increase of SOA_M tracer concentrations during spring was also observed in the southeastern United States (Ding *et al.* 2008), resulting from the enhancement of monoterpenes emission in spring (Kim et al., 2011). From May to July 2013 (period 3), SOA_M tracer concentrations were relative stable, and there was no correlation of SOA_M tracers with γ_T or SOA yield (p>0.05). These might result from the counteraction of temperature effects on emission and partitioning during the summer."(Line 277-308 in the revised manuscript)

For isoprene, the reactive uptake of epoxides onto particles plays the key role (Lin et al., 2013; Paulot et al., 2009) in isoprene SOA formation. Obviously, high temperature could enhance heterogeneous reactions and result in high levels of isoprene SOA. Figure 3a presents a negative correlation between the natural logarithm of SOA_I tracer levels and the reciprocal of temperature in Kelvin (p<0.001). Moreover, the

temperature dependence of SOA_I tracers was similar to that of C_T, and SOA_I tracers exhibited a significant positive correlation with C_T during our sampling at the NC site (Figure 3b). These results indicated that the seasonal variation of SOA_I tracers at the NC site was mainly influenced by isoprene emission.

These discussions about the seasonal variation of isoprene SOA tracers were added in the revised manuscript as "Figure 3a presents a negative correlation between the natural logarithm of SOA_I tracer levels and the reciprocal of temperature in Kelvin ($p<0.001$). Moreover, the temperature dependence of SOA_I tracers was similar to that of C_T, and SOA_I tracers exhibited a significant positive correlation with C_T during our sampling at the NC site (Figure 3b). These results indicated that the seasonal variation of SOA_I tracers at the NC site was mainly influenced by isoprene emission. Considering the short lifetime (several hours) of isoprene in the air, SOA_I should be mainly formed from local precursor. In summer, high temperature and intense light could enhance isoprene emission and photo-reactions. Moreover, high temperature in summer could enhance the heterogeneous reactions of isoprene-derived epoxides on particles which play key roles in isoprene SOA formation (Lin et al., 2013; Paulot et al., 2009). All these interpreted the high levels of isoprene SOA tracers in the summer at the NC site." (Line 230-239). Figure 3 was added in the revised manuscript.

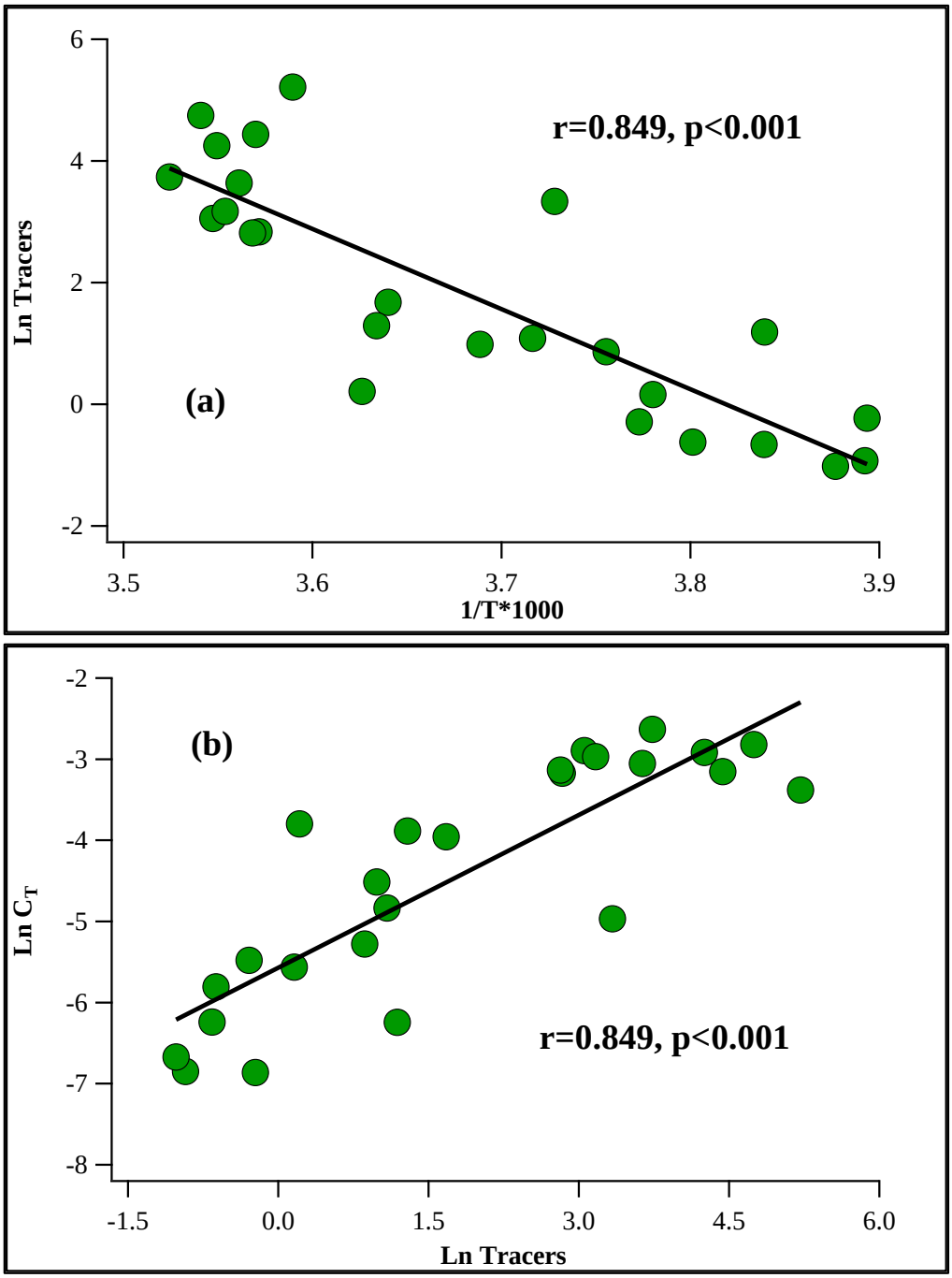

Figure 3 Correlations of SOA_I tracers with temperature (a) and C_T (b)

2. The large uncertainty of the SOA-tracer method and the simple backward trajectory analysis make the source apportionment in this work not very convincible. More detailed information about the anthropogenic emissions from Indian subcontinent and inland China would be helpful for the SOA source apportionment.

Reply: Yes, we agree. Unfortunately, emission inventories are not available in the Indian subcontinent and the Tibetan Plateau. Instead, we looked up the satellite data of population density (Socioeconomic Data and Applications Center, http://sedac.ciesin.columbia.edu/maps/gallery/search?facets=theme:population), aerosol optical thickness (AOT, NASA Earth Observations,

http://neo.sci.gsfc.nasa.gov/), tropospheric NO_2 vertical column densities (VCD, The Aura Validation Data Center, http://avdc.gsfc.nasa.gov/), and surface CO (https://www2.acd.ucar.edu/mopitt) on the global scale. As shown in Figure 4a, the northern Indian subcontinent (area within the red circle) was the most populated region of the world, with a population density of more than 1000 persons per km^2. Moreover, the plots of global AOT, tropospheric NO_2 VCD, and surface CO (Figure 4, b-d) all illustrated that the northern Indian subcontinent, including Bangladesh, Nepal, the northeastern India, and the northwestern India was the global hotspots of these anthropogenic pollutants. Compared with the northern Indian subcontinent, the Tibetan Plateau exhibited extremely low population density and low levels of AOT, surface CO, and NO_2 VCD (Figure 5, a-d). Besides these satellite data, a recent study at a site in the northwestern India (Indo-Gangetic plain) witnessed extremely high levels (up to 2065 ng m^{-3}) of polycyclic aromatic hydrocarbons which were mainly from anthropogenic combustion processes (Dubey et al., 2015). All these demonstrated that there were high anthropogenic emissions in the northern India subcontinent.

In the revised manuscript, we added the discussions about the anthropogenic emissions in the India subcontinent (see below). Figure 4 and 5 were added in the supplemental information file and the revised manuscript as Figure S7 and Figure 8, respectively.

"To check the potential source areas of anthropogenic emissions, the satellite data of population density (http://sedac.ciesin.columbia.edu/theme/population), aerosol optical thickness (AOT, http://neo.sci.gsfc.nasa.gov/), tropospheric NO_2 vertical column densities (VCD, http://avdc.gsfc.nasa.gov/), and surface CO (https://www2.acd.ucar.edu/mopitt) were analysis on the global scale. As shown in Figure S7a, the northern Indian subcontinent was the most populated region of the world, with a population density of more than 1000 persons per km^2. Moreover, the plots of global AOT, tropospheric NO_2 VCD, and surface CO (Figure S7, b-d) illustrated that the northern Indian subcontinent, including Bangladesh, Nepal, the northeastern India, and the northwestern India was the global hotspots of these anthropogenic pollutants. Compared with the northern Indian subcontinent, the TP exhibited extremely low population density and low levels of AOT, surface CO, and NO_2 VCD (Figure 8, a-d). Besides these satellite data, a recent study at a site in the northwestern India (Indo-Gangetic plain) witnessed extremely high levels (up to 2065 ng m-3) of polycyclic aromatic hydrocarbons which were mainly from anthropogenic combustion processes (Dubey et al., 2015). All these demonstrated that there were high anthropogenic emissions in the northern India subcontinent." (Line 350-364)

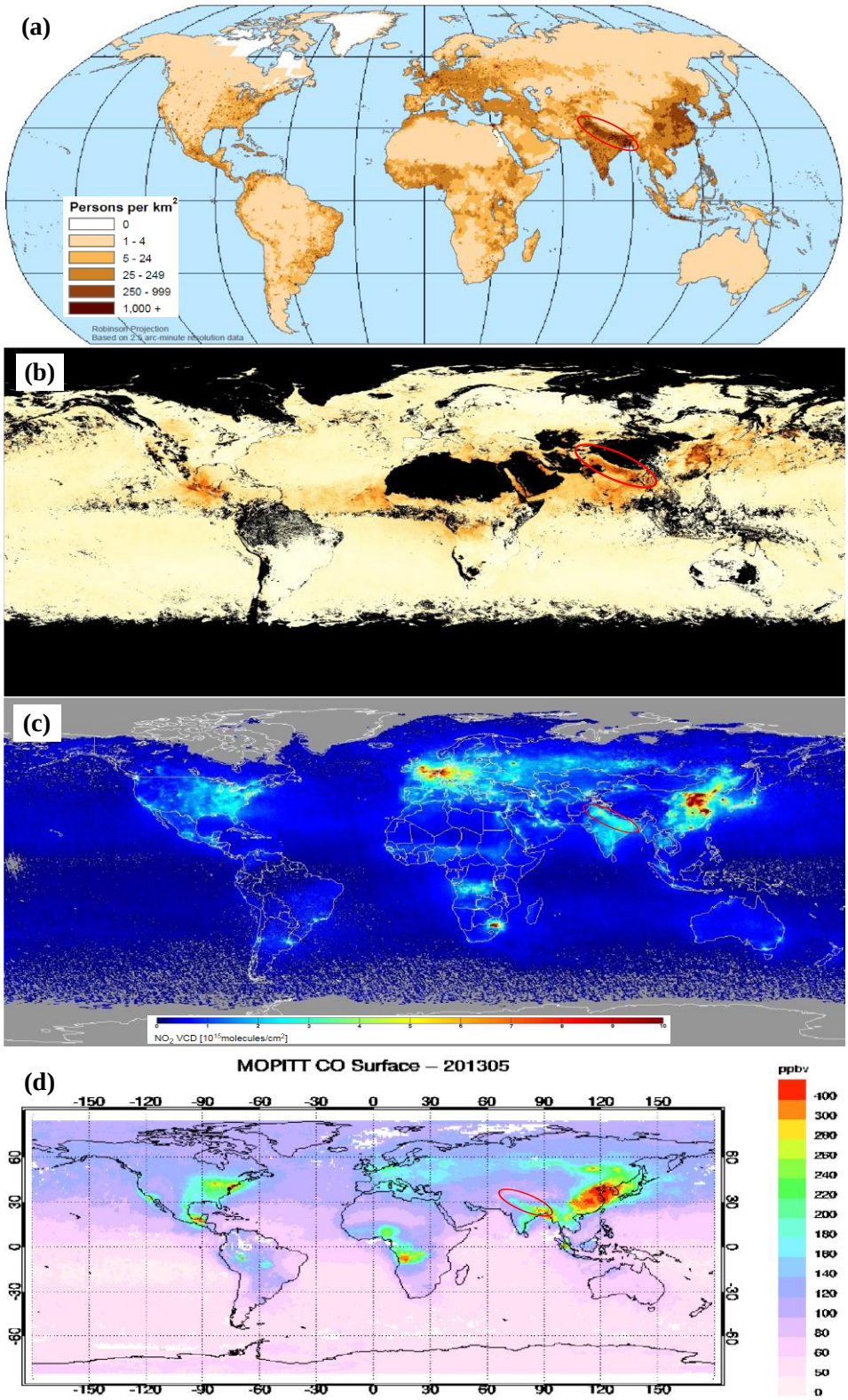

Figure 4 Global distribution of population density in 2000 (a), AOT (b), tropospheric NO_2 VCD (b), and surface CO (d) in May 2013. The area within the red circle is the northern India subcontinent.

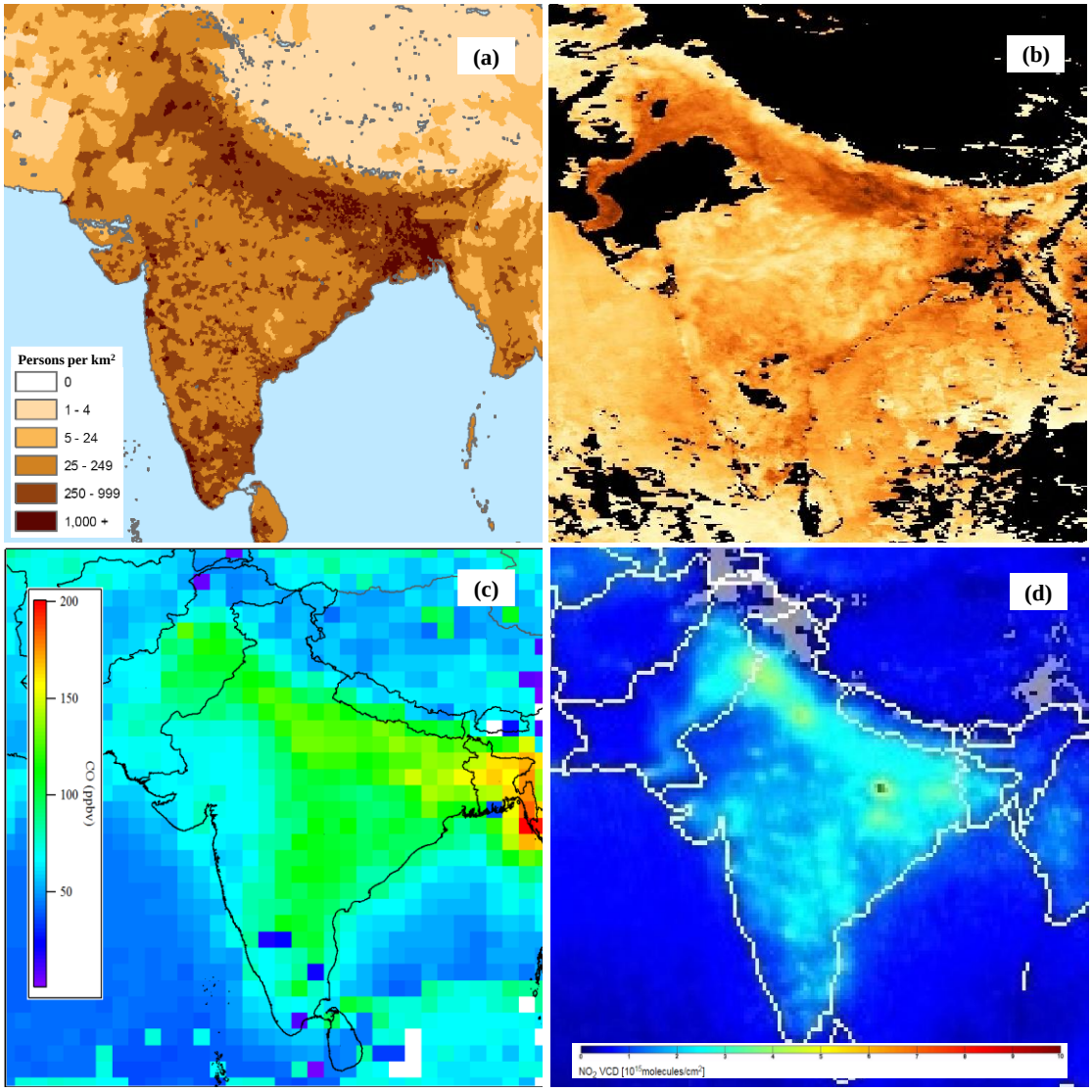

Figure 5 Distribution of population density in 2000 (a), AOT (b), surface CO (c), and NO_2 VCD (d) in May 2013 over the Indian subcontinent and the TP.

References

Dubey, J., Maharaj Kumari, K., and Lakhani, A.: Chemical characteristics and mutagenic activity of PM2.5 at a site in the Indo-Gangetic plain, India, Ecotoxicol. Environ. Saf., 114, 75-83, 2015.

Guenther, A. B., Zimmerman, P. R., Harley, P. C., Monson, R. K., and Fall, R.: Isoprene and monoterpene emission rate variability: Model evaluations and sensitivity analyses, J. Geophys. Res.-Atmos., 98, 12609-12617, 1993.

Lin, Y.-H., Zhang, H., Pye, H. O. T., Zhang, Z., Marth, W. J., Park, S., Arashiro, M., Cui, T., Budisulistiorini, S. H., Sexton, K. G., Vizuete, W., Xie, Y., Luecken, D. J., Piletic, I. R., Edney, E. O., Bartolotti, L. J., Gold, A., and Surratt, J. D.: Epoxide as a precursor to secondary organic aerosol formation from isoprene photooxidation in the presence of nitrogen oxides, Proc. Natl. Acad. Sci. U. S. A., 110, 6718-6723, 2013.

Ming, J., Xiao, C., Sun, J., Kang, S., and Bonasoni, P.: Carbonaceous particles in the atmosphere and precipitation of the Nam Co region, central Tibet, J. Environ. Sci., 22,

1748-1756, 2010.
Odum, J. R., Hoffmann, T., Bowman, F., Collins, D., Flagan, R. C., and Seinfeld, J. H.: Gas/particle partitioning and secondary organic aerosol yields, Environ. Sci. Technol., 30, 2580-2585, 1996.
Paulot, F., Crounse, J. D., Kjaergaard, H. G., Kürten, A., St. Clair, J. M., Seinfeld, J. H., and Wennberg, P. O.: Unexpected epoxide formation in the gas-phase photooxidation of isoprene, Science, 325, 730-733, 2009.
Sheehan, P. E., and Bowman, F. M.: Estimated effects of temperature on secondary organic aerosol concentrations, Environ. Sci. Technol., 35, 2129-2135, 2001.

Anonymous Referee #2

The manuscript presents new measurements of SOA tracers in the Central Tibetan Plateau and discusses seasonal variations in the absolute and relative contributions of biogenic and SOA tracers, particularly in the context of air mass origins. The manuscript requires major revisions prior to reconsideration for publication, namely in the broader discussion of potential local influences on SOA formation, the stability of the utilized tracers during transport, and the specificity and representativeness of a single toluene-SOA tracer to represent all of anthropogenic SOA. Analytically, differences between the methods utilized here and prior studies (e.g. Kleindienst et al. 2007) introduce complications and biases to the use of the SOA-tracer based source apportionment method. These biases, as well as others in quantification stemming from the use of surrogate quantification standards and an extraction protocol giving 65% recovery at times, need to be discussed and quantitatively assessed in order to develop realistic estimates of the errors in absolute quantification of SOA tracers.

Specific comments are provided here:

1. The title should be revised – "tracers" should be added after "secondary organic aerosol" in order to clarify that a select sub-set of SOA tracers were measured, and SOA in its entirety is not discussed. Also suggest removing "Nam Co" from the title to make it more concise.

Reply: The title has been revised as "Seasonal variation of secondary organic aerosol tracers in Central Tibetan Plateau"

2. The authors attribute SOA to long-range transport, but to not address the potential for SOA to form from local VOC precursors or combustion activities. The potential for release of biogenic VOC from nearby vegetation and NOx from local combustion sources (e.g. dung or biomass burning) must be addressed (Duo et al. 2015; Xiao et al. 2015).

Reply: Our study found that the seasonal variation of isoprene SOA (SOA_I) tracers was mainly influenced by the isoprene emission (C_T) which was estimated using local temperature. Considering the short lifetime of isoprene in the air (several hours), SOA_I should be mainly formed from local precursor. For monoterpene SOA (SOA_M), the ratio of *cis*-pinonic acid plus pinic acid to 3-methyl-1,2,3-butanetricarboxylic acid (P/M) indicated that SOA_M was generally fresh at the NC site (see the details in our reply to comment #12). Thus, SOA_M should be also mainly formed from local precursors. The local dung or biomass burning may be potential sources of aromatics, NOx, and even biogenic VOCs. However, the biomass burning tracer, levoglucosan not only exhibited different seasonal trend away from SOA tracers (Figure 6), but also presented poor correlations with all SOA tracers ($p>0.05$). These suggested that local dung or biomass burning was not the major sources of SOA during our sampling at the NC site.

For aromatic SOA (SOA_A), its tracer, DHOPA exhibited higher levels when air masses mainly came from the upwind Indian subcontinent (the Bangladesh and the northeastern India) where high population density and high levels of anthropogenic pollutants (AOT, CO, N_2O) were observed (see our response to the second comment by Reviewer #1). Considering there was few local anthropogenic source near the remote NC site, SOA_A should be not locally formed but mainly long-range transported from the upwind Indian subcontinent.

In the revised manuscript, we addressed that SOA_I and SOA_M were mainly formed from

local precursors, and SOA_A was from long-range transport from the upwind Indian subcontinent. The impact of local biomass burning was also discussed (see below).

"Figure 3a presents a negative correlation between the natural logarithm of SOA_I tracer levels and the reciprocal of temperature in Kelvin ($p<0.001$). Moreover, the temperature dependence of SOA_I tracers was similar to that of C_T, and SOA_I tracers exhibited a significant positive correlation with C_T during our sampling at the NC site (Figure 3b). These results indicated that the seasonal variation of SOA_I at the NC site was mainly influenced by the isoprene emission. Considering the short lifetime (several hours) of isoprene in the air, SOA_I should be mainly formed from local precursor."(Line 230-235)

"In this study, the ratio of P/M averaged 16.7 ± 20.9. Thus, SOA_M was generally fresh at the NC site and should be mainly formed from local precursors." (Line 317-319)

"Besides urban emissions from solvent and fossil fuel use, biomass burning is an important source of aromatics in many parts of the world (Lewis et al. 2013). The local dung or biomass burning (Duo et al. 2015; Xiao et al. 2015) may be potential sources of aromatics in the TP. Hence, DHOPA may come from the processing of biomass burning emissions. Figure 7 exhibits the monthly variation of biomass burning tracer, levoglucosan during our sampling. The concentrations of levoglucosan ranged from 0.82 ng m^{-3} (October 2012) to 4.55 ng m^{-3} (April 2013) with a mean of 1.87 ± 1.14 ng m^{-3}. Apparently, the monthly variation trend of levoglucosan was quite different from that of DHOPA. And there was no correlation between DHOPA and levoglucosan ($p>0.05$) (Figure S6). These indicated that DHOPA was not mainly from the processing of biomass burning emission at the NC site. Since there was few anthropogenic source near the remote NC site, the SOA_A tracer should be not locally formed but mainly transported from upwind regions." (Line 339-349)

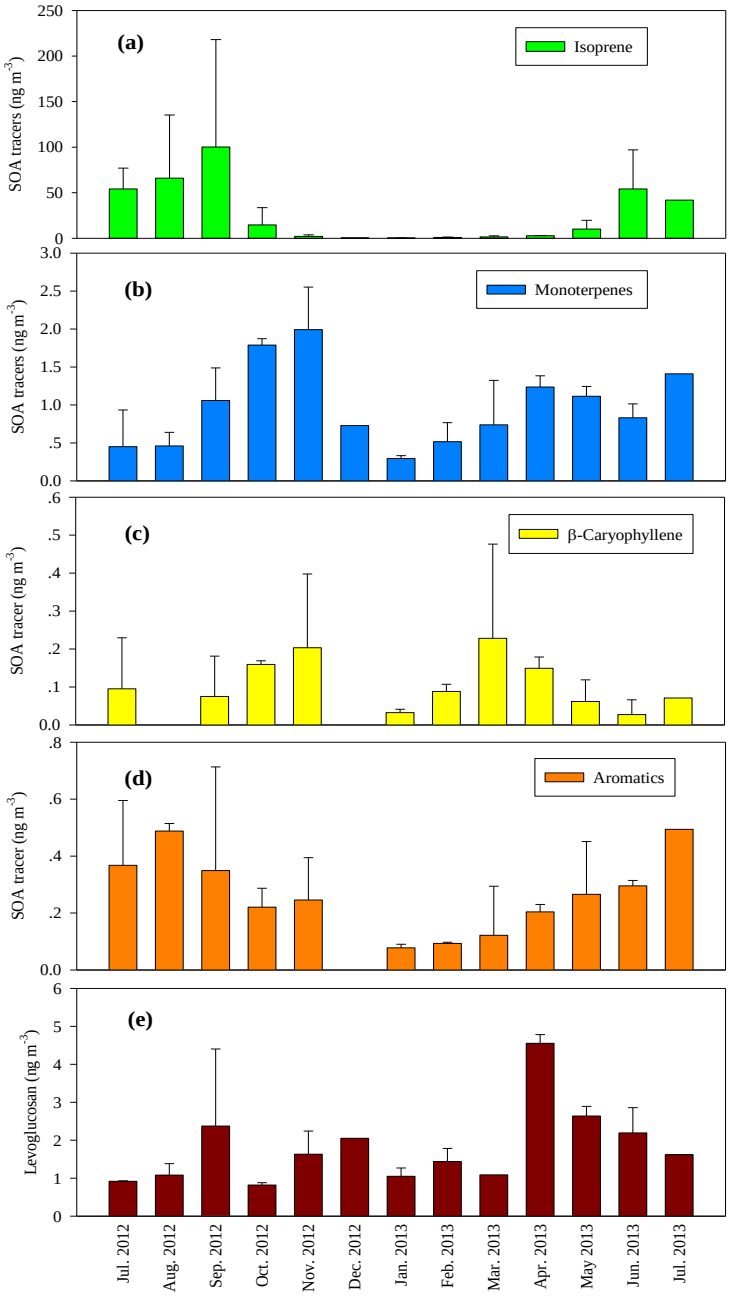

Figure 6 Monthly variations of SOA tracers (a-d) and levoglucosan (e)

3. Related, to what extent are the measured SOA tracers stable over the distance and time suggested for long-range transport? Prior studies have demonstrated extensive processing of organic aerosols in the region (Meng et al. 2013) as well as the loss of molecular tracers for organic aerosol during long-range transport (Stone et al. 2007).

Reply: The stability of SOA tracers during long-range transport is an interesting topic. Due to dilution, deposition and aging, the concentrations of SOA tracers should significantly decline during long-range transport. As we mentioned above, the biogenic SOA was mainly formed from local emissions. Thus, the concentrations of SOA_I tracers (up to184 ng m^{-3}) at the NC site were comparable with those over continents (several to hundreds ng m^{-3}). On the contrary, since SOA_A was mainly transported from the upwind Indian subcontinent, even the highest

concentration of DHOPA at the NC site was 1-2 orders of magnitude lower than those reported in the urban regions of the world. The global lifetimes of aerosols in the air are about 5 days (Bourgeois and Bey, 2011). Due to low temperature, the lifetimes of aerosols should be longer in cold regions, such as the Arctic and the Tibetan Plateau. At present, there is no result available in the lifetimes of these SOA tracers in the ambient air. We think the lifetimes of SOA tracers over the Tibetan Plateau should be comparable with those of aerosols. Given a lifetime of 5 days, the loss rate constant of tracers could be roughly estimated as 2.3×10^{-12} cm^3 $molec^{-1}$ s^{-1} at OH levels of 1×10^6 molecules cm^{-3}. This is also the reason why we run back trajectory analysis only for 5 days.

Bourgeois, Q., and Bey, I.: Pollution transport efficiency toward the Arctic: Sensitivity to aerosol scavenging and source regions, J. Geophys. Res.-Atmos., 116, D08213, Doi: 10.1029/2010JD015096, 2011.

4. Section 2.2: Specify what type of ionization was used by the mass spectrometer
Reply: Electron impact (EI) ionization was used by the mass spectrometer. We have specified it in the revised manuscript "Thirteen SOA tracers were quantified by the GC-MS coupled with an electron impact (EI) ionization source" (Line 132-133)

5. Kleindienst et al. (2007) utilized chemical ionization, a soft ionization technique, to identify SOA tracers using molecular ions and high-m/z ratios, and analyzed SOA chamber samples in parallel to ambient samples to ensure consistency in mass fragmentation and gas chromatography (GC) retention times. Evidence in the form of retention data, observed MS fragments, and relative ratios of MS fragments are needed as evidence for the correct identification of the SOA tracer compounds. This information should be added as supplemental information.
Reply: Figure 7 presents the TIC of these SOA tracers with the retention time of each compound labeled. Figure 8-10 show the EI spectrum of each tracer. In the revised manuscript, Figure 7-10 were added in the supplemental information file as Figure S1-S4, and we mentioned these in Line 138-139 "Figure S1 presents the total ion chromatogram (TIC) of these SOA tracers." and Line 143 "The EI spectrum of each SOA tracer is shown in Figure S2-S4."

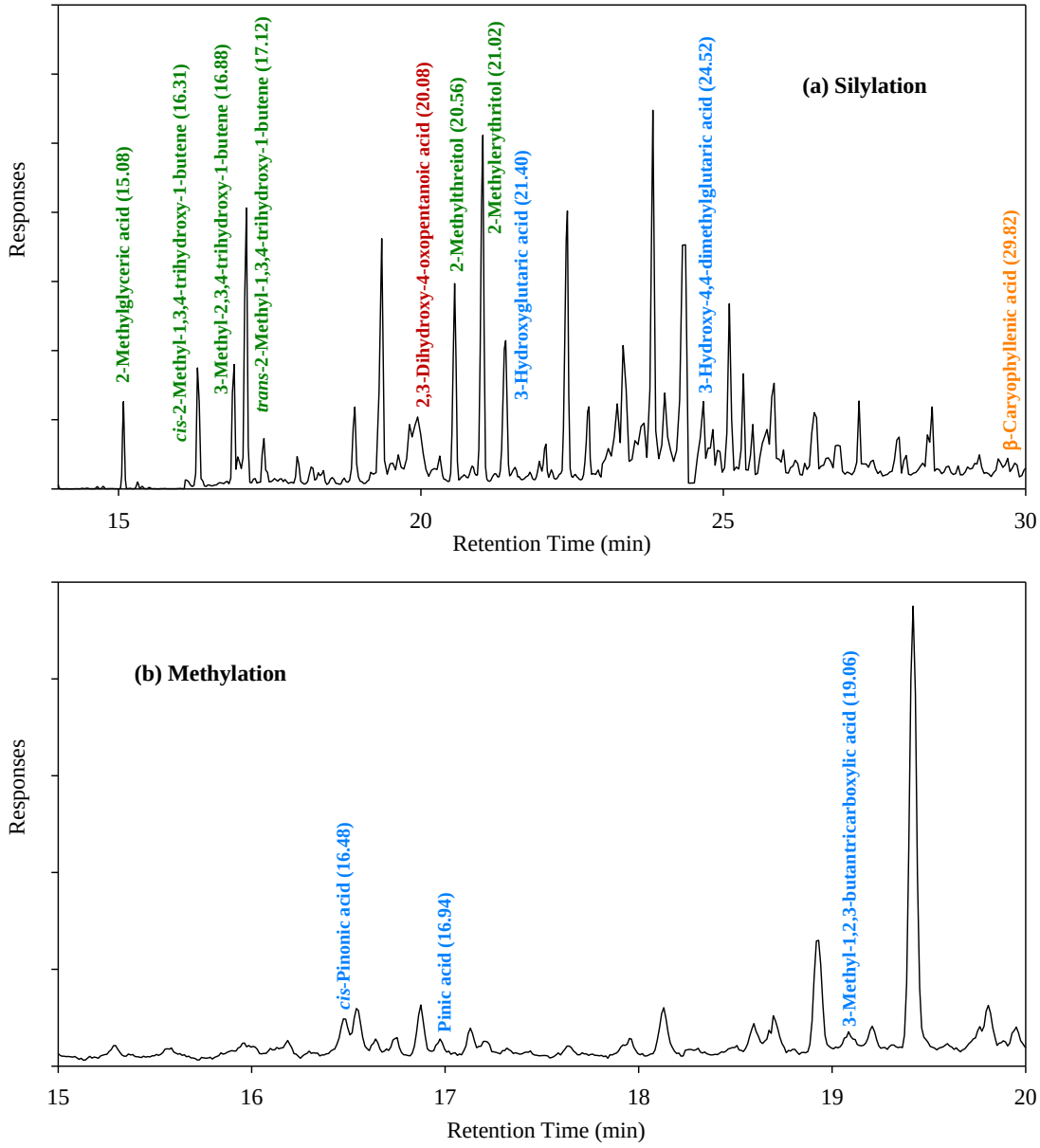

Figure 7 TIC of silylated (a) and methylated samples (b). Retention time of each tracer is labeled in brackets. Green, blue, orange and red represent SOA tracers from isoprene, monoterpenes, β-caryophyllene and aromatics, respectively.

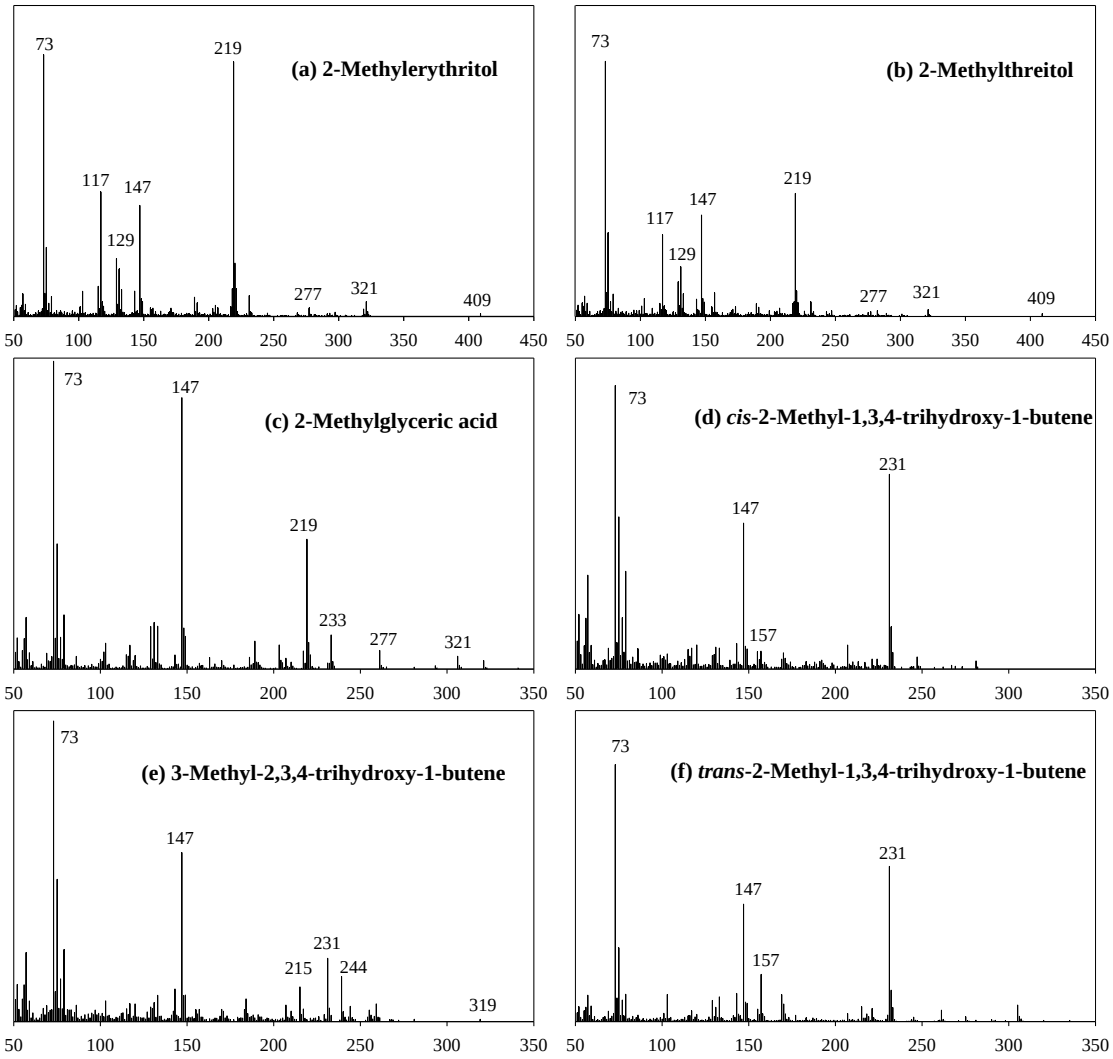

Figure 8 EI spectra of silylated isoprene SOA tracers

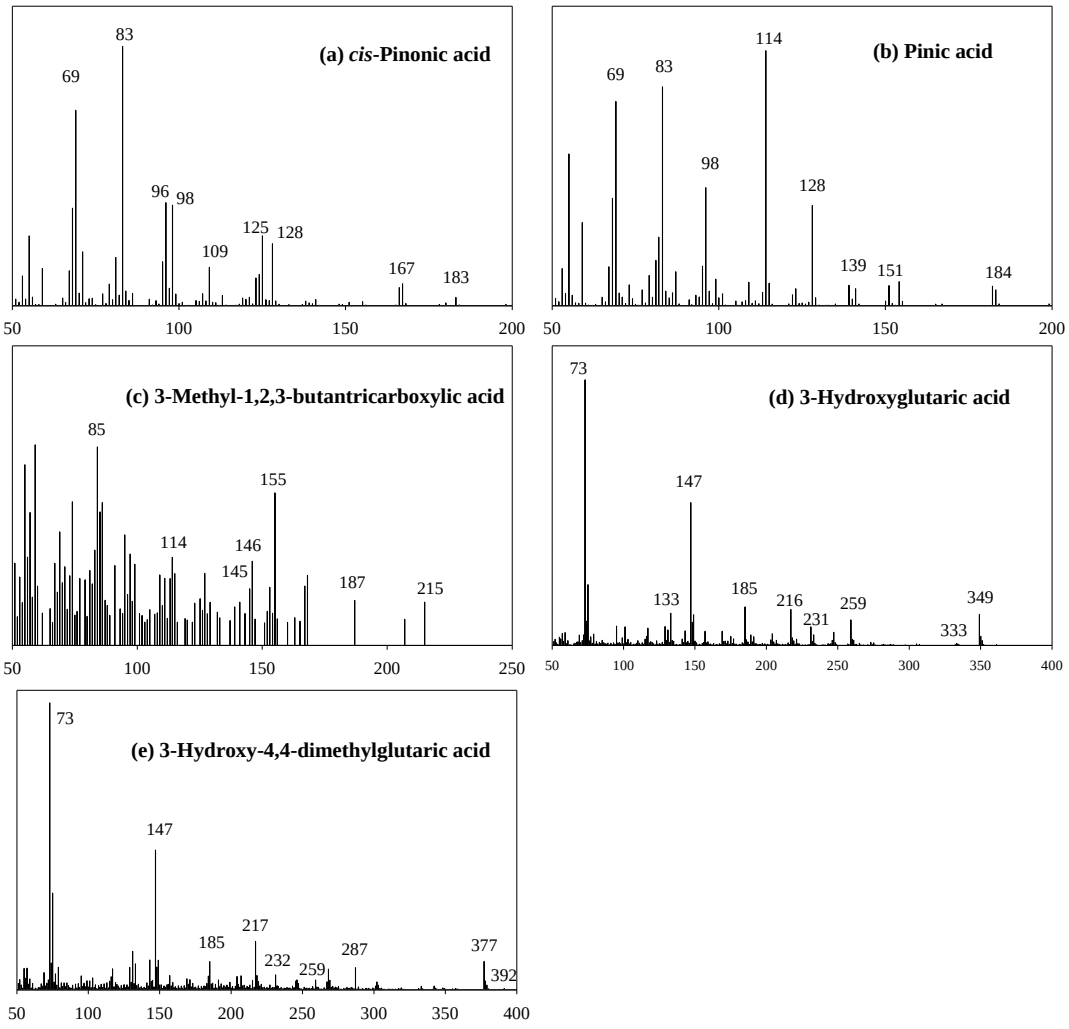

Figure 9 EI spectra of methylated (a-c) and silylated (d and e) monoterpene SOA tracers

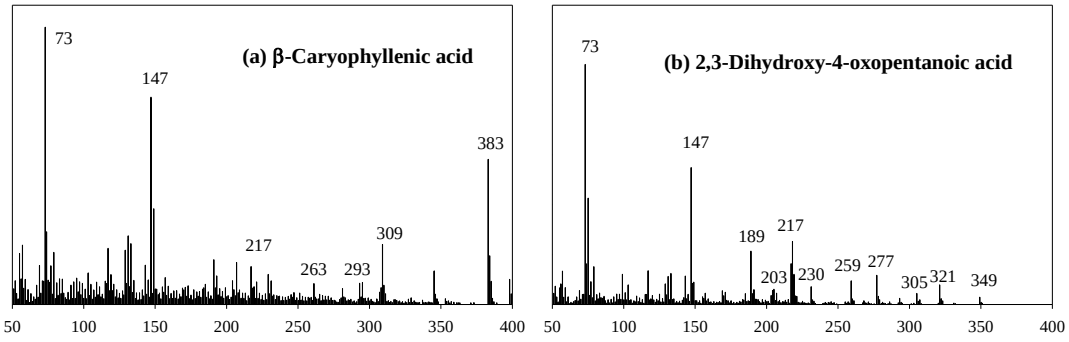

Figure 10 EI spectra of silylated SOA tracers from β-caryophyllene (a) and aromatics (b)

6. SOA tracers were quantified using surrogate standards, because analytical standards are not commercially-available for most of these compounds. The use of a surrogate standard introduces bias to the measurement, because it does not accurately represent the ionization and mass fragmentation of the target analyte. Moreover, the comparison of response factors of the

five surrogate standards (1-8 on page 7147) is irrelevant, because the issue is about the agreement of the response factors of the SOA tracers with the surrogates, not between the surrogates and each other. Consequently, the reported absolute concentrations of SOA tracers, are thus subject to large uncertainties, particularly when the structural match between the surrogate standard and analyte is poor (Stone et al. 2012). The manuscript should clearly state that presence and significance of this uncertainty and discuss the potential bias it may introduce to the results.

Reply: We appreciate the suggestion in uncertainty estimation for SOA tracer measurement. Stone et al., (2012) developed an empirical approach to estimate the error from surrogate quantification (E_Q) based on homologous series of atmospherically relevant compounds. These quantification errors (E_Q) are then propagated with the standard deviation of the field blank (E_{FB}) and error in spike recovery (E_R), and yield the measurement uncertainties (E_A) for SOA tracers. We have calculated the E_Q and E_A for SOA tracers using the method developed by Stone et al. (2012). As shown in Table 2, the errors from surrogate quantification (E_Q) ranged from 15% (2-methyltetrols) to 155% (β-caryophyllenic acid) in this study. Since SOA tracers were not detected in the field blanks, E_{FB} was 0 in this study. The spike recoveries of surrogate standards were used to estimate the E_R of tracers. The uncertainties in analyte measurement (E_A) were estimated in the range of 38% to 156%.

In the revised manuscript, we added a section "2.4 Estimation of measurement uncertainty" to discuss the uncertainty in tracer measurement (Line 159-179, also see below). Table 2 was added in the supplemental information file as Table S1.

"2.4 Estimation of measurement uncertainty

Since there is no commercial standard available for most SOA tracers (except *cis*-pinonic acid and pinic acid), the use of surrogate standards for quantification introduces additional error to measurement. Error in analyte measurement (E_A) is propagated from the standard deviation of the field blank (E_{FB}), error in spike recovery (E_R) and the error from surrogate quantification (E_Q):

$$E_A = \sqrt{{E_{FB}}^2 + {E_R}^2 + {E_Q}^2} \quad (1)$$

Since SOA tracers were not detected in the field blanks, E_{FB} was 0 in this study. The spike recoveries of surrogate standards were used to estimate the E_R of tracers which ranged from 1% (*cis*-pinonic acid) to 35% (erythritol). Stone et al. (2012) developed an empirical approach to estimate E_Q based on homologous series of atmospherically relevant compounds. The relative error introduced by each carbon atom (E_n) was estimated to be 15 %, each oxygenated functional group (E_f) to be 10% and alkenes (E_d) to be 60%. The errors introduced from surrogate quantification are treated as additive and are calculated as:

$$E_Q = E_n \Delta n + E_f \Delta \mathrm{f} + E_d \Delta \mathrm{d} \quad (2)$$

where Δn is the difference in carbon atom number between a surrogate and an analyte, Δf is the difference in oxygen-containing functional group between a surrogate and an analyte, Δd is the difference in alkene functionality between a surrogate and an analyte.

Table S1 shows the estimated uncertainties in tracer measurement. The errors from

surrogate quantification (E_Q) ranged from 15% (2-methyltetrols) to 155% (β-caryophyllenic acid) in this study. Propagated with the error in recovery, the uncertainties in analyte measurement (E_A) were estimated in the range of 38% to 156%."

Table 2 Estimation of measurement uncertainty

Tracers	**Tracer formula**	**Surrogates**	**Surrogate formula**	**E_Q (%)**	**E_R[a] (%)**	**E_A (%)**
cis-Pinonic acid	$C_{10}H_{16}O_3$	*cis*-Pinonic acid			1	
Pinic acid	$C_9H_{14}O_4$	Pinic acid			30	
3-Methyl-1,2,3-butantricarboxylic acid	$C_8H_{12}O_6$	*cis*-Pinonic acid	$C_{10}H_{16}O_3$	60	1	60
3-Hydroxyglutaric acid	$C_5H_8O_5$	*cis*-Pinonic acid	$C_{10}H_{16}O_3$	95	1	95
3-Hydroxy-4,4-dimethylglutaric acid	$C_7H_{12}O_5$	*cis*-Pinonic acid	$C_{10}H_{16}O_3$	65	1	65
cis-2-Methyl-1,3,4-trihydroxy-1-butene	$C_5H_{10}O_3$	Erythritol	$C_4H_{10}O_4$	85	35	92
3-Methyl-2,3,4-trihydroxy-1-butene	$C_5H_{10}O_3$	Erythritol	$C_4H_{10}O_4$	85	35	92
trans-2-Methyl-1,3,4-trihydroxy-1-butene	$C_5H_{10}O_3$	Erythritol	$C_4H_{10}O_4$	85	35	92
2-Methylglyceric acid	$C_4H_8O_4$	Erythritol	$C_4H_{10}O_4$	20	35	40
2-Methylthreitol	$C_5H_{12}O_4$	Erythritol	$C_4H_{10}O_4$	15	35	38
2-Methylerythritol	$C_5H_{12}O_4$	Erythritol	$C_4H_{10}O_4$	15	35	38
β-Caryophyllenic acid	$C_{13}H_{20}O_4$	Octadecanoic acid	$C_{18}H_{36}O_2$	155	17	156
2,3-Dihydroxy-4-oxopentanoic acid	$C_5H_8O_5$	Azelaic acid	$C_9H_{16}O_4$	90	11	91

[a] E_R is the difference between 100% and mean recovery of each surrogate standard.

Stone, E. A., Nguyen, T. T., Pradhan, B. B., and Dangol, P. M.: Assessment of biogenic secondary organic aerosol in the Himalayas, Environ. Chem., 9, 263-272, 2012.

7. Major issues arise when deviating from the quantification method of Kleindienst et al. (2007) for SOA tracers and using the SOA-tracer method for source apportionment. Namely, the f-SOC values (page 7154 line 15) were developed using the 5-ion quantification approach with a single-point calibration with ketopinic acid as the quantification standard and chemical ionization in the MS source. In this work, the authors have changed the MS detection method, internal standard, and surrogate standards, such that the f-SOC values cannot be directly applied. A large degree of bias is expectedly introduced, but is not quantifiable. The authors need to be realistic about the magnitude of error that this could introduce, which is likely on the order of 5-10 times different, rather than 23%.

Reply: As discuss above, we re-calculated the uncertainties in SOA tracer measurement and then re-estimated the uncertainties in SOC apportionment. Based on the E_A values in Table 1, the uncertainties in tracer analyses were up to 40% for SOA_I (only MGA and MTLs involved for SOC estimation), up to 95% for SOA_M, 156% for SOA_C, and 91% for SOA_A. The uncertainties of f_{SOC} were reported to be 25% for isoprene, 48% for monoterpenes, 22% for β-caryophyllene and 33% for aromatics. Considering these factors, the uncertainties of SOC apportionment were calculated through error propagation. The RSD were 47% for SOC_I, 106% for SOC_M, 157% for SOC_C, and 96% for SOC_A. On average, the RSD of the reconstructed SOC

(sum of the four precursors) was 51±11%.

In the revised manuscript, we addressed these as "The uncertainty in the SOA-tracer method is induced from the analysis of organic tracers and the determination of the conversion factors. Based on the E_A values in Table S1, the uncertainties in the tracer analyses were within 40% for SOA_I (only MGA and MTLs involved for SOC estimation), 95% for SOA_M, 156% for SOA_C, and 91% for SOA_A. The uncertainties of f_{SOC} were reported to be 25% for isoprene, 48% for monoterpenes, 22% for β-caryophyllene and 33% for aromatics (Kleindienst *et al.* 2007, Lewandowski *et al.* 2013). Considering these factors, the uncertainties of SOC apportionment were calculated through error propagation. The RSD were 47% for SOC_I, 106% for SOC_M, 157% for SOC_C, and 96% for SOC_A. On average, the RSD of the reconstructed SOC (sum of the four precursors) was 51±11%." (Line 426-434)

8. Revision with respect to uncertainty in SOA tracer measurements is needed in section 3.2, page 7155 line 3.

Reply: In the revised manuscript, we have re-calculated the uncertainties of SOC apportionment with respect to uncertainty in SOA tracer measurement. The RSD were 47% for SOC_I, 106% for SOC_M, 157% for SOC_C, and 96% for SOC_A. On average, the RSD of the reconstructed SOC (sum of the four precursors) was 51±11%. (See discussions above)

9. Clarify the "paired duplicate samples" described in section 2.3 line 16. Are these duplicate samples of ambient aerosol that were collected in parallel? Or were these extracts that were split and analyzed twice?

Reply: These duplicate samples were ambient aerosol that were collected in parallel. We clarify it in the revised manuscript "The relative differences for target compounds in samples collected in parallel (n=6) were all below 15%." (Line 151-152)

10. Were the absolute concentrations of SOA tracers corrected for the less than optimal recoveries reported in section 2.3? Or is this another source of error in the ambient measurements?

Reply: No, the absolute concentrations of SOA tracers did not correct using recoveries. The recoveries of target compounds ranged from 65% (erythritol) to 101% (*cis*-pinonic acid), suggesting that the errors in analyte recovery should be within 35% in this study. In the revised manuscript, the recovery data were used to calculate the errors in analyte recovery (E_R) for SOA tracers (See Table 1). Then, uncertainties in SOA tracer measurement (E_A) were estimated through error propagation from E_R and the error from surrogate quantification (E_Q).

11. The sentence on page 7149 (lines 9-10) should be moved to follow the description of the model.

Reply: In the revised manuscript, we moved the sentence to follow the description of the model (Line 230-231).

12. The authors should work towards developing a deeper discussion of the monoterpene SOA tracers using knowledge of first and multi-generation oxidation products of monoterpenes (Glasius et al. 2000; Jaoui et al. 2005; Szmigielski et al. 2007) and reaction pathways

(Eddingsaas et al. 2012) as has been done for isoprene.

Reply: We appreciate the suggestion. Previous study proposed that *cis*-pinonic acid and pinic acid were the first-generation products of SOA_M, and only formed under low-NOx conditions (Eddingsaas et al. 2012). The dominance of *cis*-pinonic acid and pinic acid among SOA_M tracers at the remote NC site indicated that SOA_M there was mainly formed under low-NOx conditions. Moreover, *cis*-pinonic acid and pinic acid (P) could be further photo-degraded to higher-generation products, e.g. 3-methyl-1,2,3-butanetricarboxylic acid (M) (Glasius et al. 2000; Jaoui et al. 2005; Szmigielski, et al., 2007). And the ratio of *cis*-pinonic acid plus pinic acid to 3-methyl-1,2,3-butanetricarboxylic acid (P/M) could be applied to trace the aging of SOA_M (Ding et al., 2011; Gómez-González et al., 2012). In the fresh chamber produced α-pinene SOA samples, the ratios of P/M were reported in the range of 1.51 to 3.21 (Offenberg, et al., 2007). In this study, the ratio of P/M averaged 16.7 ±20.9. Thus, SOA_M was generally fresh at the NC site. Figure 11 presents a negative correlation between P/M and temperature (r=-0.560, p=0.008). Since temperature has positive influence on photo-reaction rates, the higher temperature during the summer could accelerate the photochemistry in the air and result in P to M conversion being more efficient. Thus, SOA_M in the summer was more aged than that in the winter.

We added Figure 11 in the revised manuscript (as Figure 6) to show the negative correlation between P/M and temperature, and addressed the discussions above "Previous study proposed that *cis*-pinonic acid and pinic acid (P) were the first-generation products of SOA_M and only formed under low-NOx conditions (Eddingsaas et al. 2012). The dominance of *cis*-pinonic acid and pinic acid among SOA_M tracers at the remote NC site indicated that SOA_M there was mainly formed under low-NOx conditions. Moreover, *cis*-pinonic acid and pinic acid could be further photo-degraded to higher-generation products, e.g. 3-methyl-1,2,3-butanetricarboxylic acid (M) (Glasius et al. 2000; Jaoui et al. 2005; Szmigielski, et al., 2007). And the ratio of *cis*-pinonic acid plus pinic acid to 3-methyl-1,2,3-butanetricarboxylic acid (P/M) could be applied to trace the aging of SOA_M (Ding et al., 2011; Gómez-González et al., 2012). In the fresh chamber produced α-pinene SOA samples, the ratios of P/M were reported in the range of 1.51 to 3.21 (Offenberg, et al., 2007). In this study, the ratio of P/M averaged 16.7 ±20.9. Thus, SOA_M was generally fresh at the NC site and should be mainly formed from local precursors. Figure 6 presents a negative correlation between P/M and temperature (r=-0.560, p=0.008). Higher P/M ratios were observed in the fall and the winter, and lower P/M ratios occurred in the spring and the summer. Since temperature has positive influence on photo-reaction rates, the higher temperature during the summer could accelerate the photochemistry in the air and result in P to M conversion being more efficient. Thus, SOA_M in the summer was more aged than that in the winter." (Line 309-324)

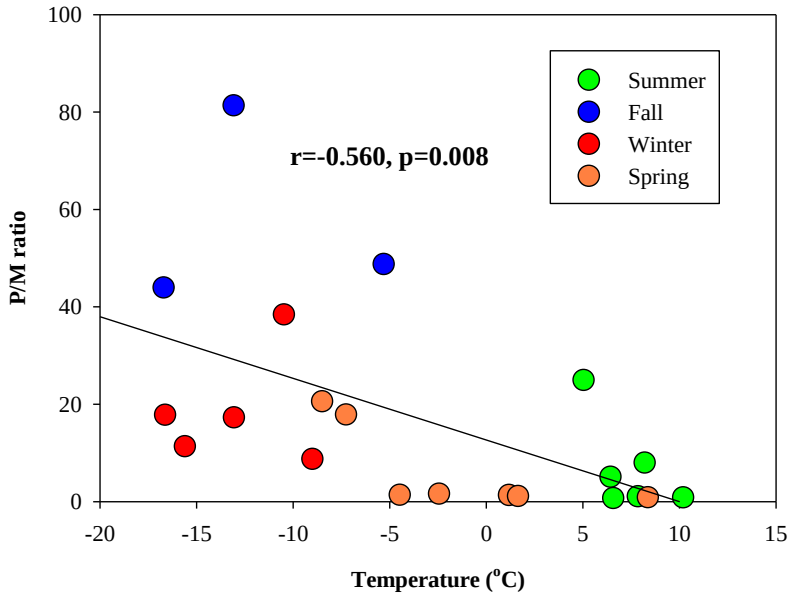

Figure 11 Negative correlation between P/M ratio and temperature

Ding, X., Wang, X., and Zheng, M.: The influence of temperature and aerosol acidity on biogenic secondary organic aerosol tracers: Observations at a rural site in the central Pearl River Delta region, South China, Atmos. Environ., 45, 1303-1311, 2011.

Eddingsaas, N. C., Loza, C. L., Yee, L. D., Chan, M., Schilling, K. A., Chhabra, P. S., Seinfeld, J. H., and Wennberg, P. O.: α-pinene photooxidation under controlled chemical conditions – Part 2: SOA yield and composition in low- and high-NOx environments, Atmos. Chem. Phys., 12, 7413-7427, 2012.

Gómez-González, Y., Wang, W., Vermeylen, R., Chi, X., Neirynck, J., Janssens, I. A., Maenhaut, W., and Claeys, M.: Chemical characterisation of atmospheric aerosols during a 2007 summer field campaign at Brasschaat, Belgium: sources and source processes of biogenic secondary organic aerosol, Atmos. Chem. Phys., 12, 125-138, 2012.

Glasius, M., Lahaniati, M., Calogirou, A., Di Bella, D., Jensen, N. R., Hjorth, J., Kotzias, D., and Larsen, B. R.: Carboxylic acids in secondary aerosols from oxidation of cyclic monoterpenes by ozone, Environ. Sci. Technol., 34, 1001-1010, 2000.

Jaoui, M., Kleindienst, T. E., Lewandowski, M., Offenberg, J. H., and Edney, E. O.: Identification and quantification of aerosol polar oxygenated compounds bearing carboxylic or hydroxyl groups. 2. Organic tracer compounds from monoterpenes, Environ. Sci. Technol., 39, 5661-5673, 2005.

Offenberg, J. H., Lewis, C. W., Lewandowski, M., Jaoui, M., Kleindienst, T. E., and Edney, E. O.: Contributions of toluene and α-pinene to SOA formed in an irradiated toluene/α-pinene/NOx/ air mixture: Comparison of results using ^{14}C content and SOA organic tracer methods, Environ. Sci. Technol., 41, 3972-3976, 2007.

Szmigielski, R., Surratt, J. D., Gómez-González, Y., Veken, P. V. d., Kourtchev, I., Vermeylen, R., Blockhuys, F., Jaoui, M., Kleindienst, T. E., Lewandowski, M., Offenberg, J. H., Edney, E. O., Seinfeld, J. H., Maenhaut, W., and Claeys, M.: 3-Methyl-1,2,3-butanetricarboxylic acid: An atmospheric tracer for terpene secondary organic aerosol, Geophys. Res. Lett., 34, L24811,

10.1029/2007GL031338, 2007.

13. The conclusion that biogenic SOC "dominated over anthropogenic SOC" is not robust, in part because only a single organic molecule is being used as a tracer of anthropogenic VOC – DHOPA. The specificity of DHOPA to anthropogenic sources is not fully established (Kleindienst et al. 2004). For example, biomass burning is a major source of toluene in many parts of the world (Lewis et al. 2013). Hence, DHOPA may be an indicator of the processing of biomass burning emissions, and not a measure of urban pollutants from solvent and fossil fuel use. The limitations of using a single, and potentially non-specific tracer for anthropogenic SOA must be discussed and the conclusions restated.

Reply: Our data suggested that biogenic SOC dominated over aromatic SOC (SOC_A). DHOPA has been widely used to access the aromatic SOA in the United States (Kleindienst et al. 2007, Stone et al. 2009, Lewandowski et al. 2013), and China (Hu et al. 2008, Guo et al. 2012, Peng et al. 2013, Ding et al. 2014). Since aromatics are mainly emitted from anthropogenic sources, and are major anthropogenic SOA precursors, we think aromatic SOA can reflect the majority of anthropogenic SOA. We admit there are limitations using a single tracer for anthropogenic SOA. In the revised manuscript, we changed the conclusion "biogenic SOC dominated over anthropogenic SOC" to "biogenic SOC dominated over SOC_A" (Line 452)

We did measure biomass burning tracer, levoglucosan in our samples. As shown in Figure 12, the monthly variation trend of levoglucosan was quite different from that of DHOPA. And there was no correlation between DHOPA and levoglucosan ($p>0.05$) at the NC site (Figure 13). These indicated that DHOPA was not mainly from the processing of biomass burning emission at the NC site. As discussed in the ACPD manuscript, the higher levels of DHOPA existed when air masses mainly came from the upwind Indian subcontinent (the Bangladesh and the northeastern India) where high population density and high levels of anthropogenic pollutants (AOD, CO, and N_2O) were observed (See our response to the second comment by Reviewer #1). Thus, we believe DHOPA observed in this study should be not mainly from local biomass burning but from long-range transport.

In the revised manuscript, we addressed these "Besides urban emissions from solvent and fossil fuel use, biomass burning is an important source of aromatics in many parts of the world (Lewis et al. 2013). The local dung or biomass burning (Duo et al. 2015; Xiao et al. 2015) may be potential sources of aromatics in the TP. Hence, DHOPA may come from the processing of biomass burning emissions. Figure 7 exhibits the monthly variation of biomass burning tracer, levoglucosan during our sampling. The concentrations of levoglucosan ranged from 0.82 ng m^{-3} (October 2012) to 4.55 ng m^{-3} (April 2013) with a mean of 1.87 ± 1.14 ng m^{-3}. Apparently, the monthly variation trend of levoglucosan was quite different from that of DHOPA. And there was no correlation between DHOPA and levoglucosan ($p>0.05$) (Figure S6). These indicated that DHOPA was not mainly from the processing of biomass burning emission at the NC site. Since there was few anthropogenic source near the remote NC site, the SOA_A tracer should be not locally formed but mainly transported from upwind regions." (Line 339-349). Figure 12b and Figure 13 were added in the revised manuscript (as Figure 7) and the supplemental information file (as Figure S6), respectively.

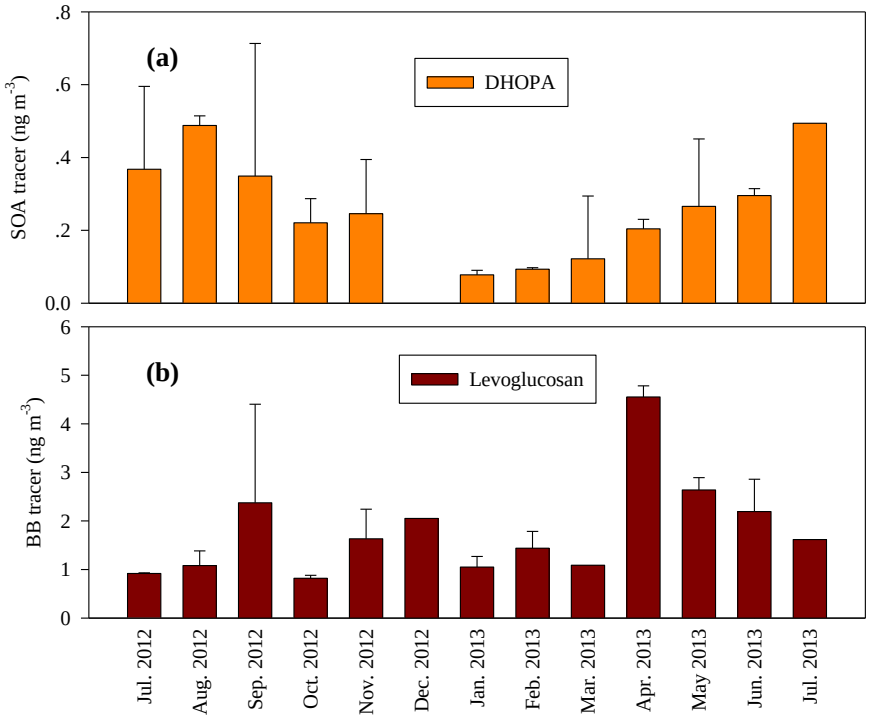

Figure 12 Monthly variations of DHOPA (a) and levoglucosan (b)

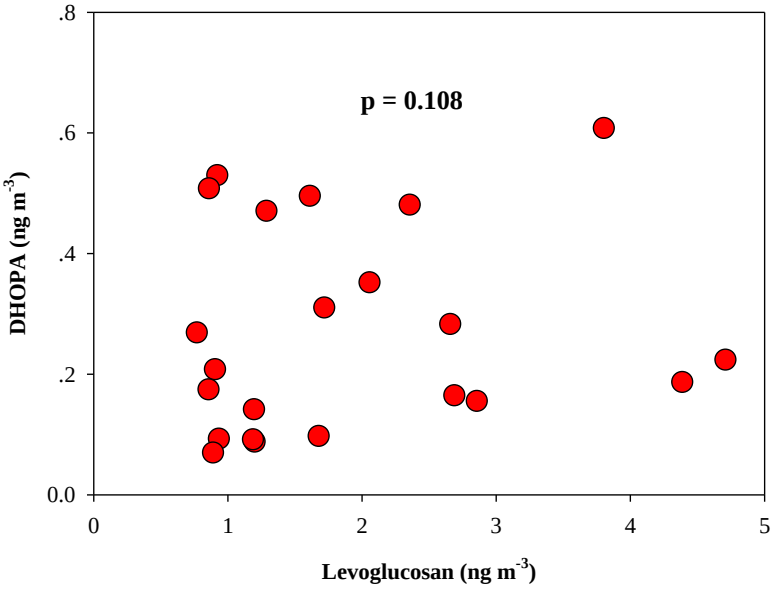

Figure 13 Scatter plot of DHOPA and levoglucosan

Kleindienst, T. E., Jaoui, M., Lewandowski, M., Offenberg, J. H., Lewis, C. W., Bhave, P. V., and Edney, E. O.: Estimates of the contributions of biogenic and anthropogenic hydrocarbons to secondary organic aerosol at a southeastern US location, Atmos. Environ., 41, 8288-8300, 2007.

Stone, E. A., Zhou, J., Snyder, D. C., Rutter, A. P., Mieritz, M., and Schauer, J. J.: A comparison of summertime secondary organic aerosol source contributions at contrasting urban locations, Environ. Sci. Technol., 43, 3448-3454, 2009.

Lewandowski, M., Piletic, I. R., Kleindienst, T. E., Offenberg, J. H., Beaver, M. R., Jaoui, M., Docherty, K. S., and Edney, E. O.: Secondary organic aerosol characterisation at field sites across the United States during the spring-summer period, Int. J. Environ. Anal. Chem., 93, 1084-1103, 2013.
Hu, D., Bian, Q., Li, T. W. Y., Lau, A. K. H., and Yu, J. Z.: Contributions of isoprene, monoterpenes, β-caryophyllene, and toluene to secondary organic aerosols in Hong Kong during the summer of 2006, J. Geophys. Res.-Atmos., 113, D22206, DOI: 10.1029/2008jd010437, 2008.
Guo, S., Hu, M., Guo, Q., Zhang, X., Zheng, M., Zheng, J., Chang, C. C., Schauer, J. J., and Zhang, R.: Primary sources and secondary formation of organic aerosols in Beijing, China, Environ. Sci. Technol., 46, 9846-9853, 2012.
Ding, X., He, Q.-F., Shen, R.-Q., Yu, Q.-Q., and Wang, X.-M.: Spatial distributions of secondary organic aerosols from isoprene, monoterpenes, β-caryophyllene, and aromatics over China during summer, J. Geophys. Res.-Atmos., 119, 11877-11891, 2014.
Peng, J. L., Li, M., Zhang, P., Gong, S. Y., Zhong, M. A., Wu, M. H., Zheng, M., Chen, C. H., Wang, H. L., and Lou, S. R.: Investigation of the sources and seasonal variations of secondary organic aerosols in PM2.5 in Shanghai with organic tracers, Atmos. Environ., 79, 614-622, 2013.

14. Clarification needed on page 7154 line 11-12 – What specifically has been done to show that the SOA tracer approach provides "reasonable results"?

Reply: Previous studies have compared the estimated SOC by SOA-tracer method and other techniques. Lewandowski et al. (2008) found that the measured OC in the midwestern United States could be fully explained by primary OC from chemical mass balance (CMB) model plus SOC from the SOA-tracer method, suggesting that the secondary organic tracer technique could be a valuable method for SOC estimation. Kleindienst et al. (2010) further compared the estimated SOC by the SOA-tracer method and other four independent methods (multiple regressions, CMB, carbon isotope and EC-tracer) in the southeastern United States, and found that these five methods matched well. Our previous study in the Pearl River Delta, south China found SOC levels estimated by the SOA-tracer method were not only consistent with but also correlated well with those by EC-tracer method in summer, (Ding et al., 2012). The SOC apportionment results were also comparable between the SOA-tracer method and the positive matrix factorization (PMF) model in Hong Kong (Hu et al. 2010). All these demonstrate that the SOA tracer approach can provide reasonable results.

In the revised manuscript, we added these statements to show that the SOA tracer approach provides reasonable results. "Lewandowski et al. (2008) found that the measured OC in the midwestern United States could be fully explained by primary OC from chemical mass balance (CMB) model plus SOC from the SOA-tracer method, suggesting that the secondary organic tracer technique could be a valuable method for SOC estimation. Kleindienst et al. (2010) further compared the estimated SOC by the SOA-tracer method and other four independent methods (multiple regressions, CMB, carbon isotope and EC-tracer) in the southeastern United States and found that these five methods matched well. Our previous study in the Pearl River Delta found SOC levels estimated by the SOA-tracer method were not only consistent with but also correlated well with those by EC-tracer method in summer, (Ding et al., 2012). The SOC apportionment results were also comparable between the SOA-tracer method and positive matrix factorization (PMF) model in Hong Kong (Hu et al. 2010)." (Line 402-412)

Ding, X., Wang, X., Gao, B., Fu, X., He, Q., Zhao, X., Yu, J., and Zheng, M.: Tracer based estimation of secondary organic carbon in the Pearl River Delta, South China, J. Geophys. Res.-Atmos., 117, D05313, doi: 10.1029/2011JD016596, 2012.
Hu, D., Bian, Q., Lau, A. K. H., and Yu, J. Z.: Source apportioning of primary and secondary organic carbon in summer $PM_{2.5}$ in Hong Kong using positive matrix factorization of secondary and primary organic tracer data, J. Geophys. Res.-Atmos., 115, D16204, doi: 10.1029/2009JD012498, 2010.
Kleindienst, T. E., Lewandowski, M., Offenberg, J. H., Edney, E. O., Jaoui, M., Zheng, M., Ding, X., and Edgerton, E. S.: Contribution of primary and secondary sources to organic aerosol and PM2.5 at SEARCH network sites, J. Air & Waste Manage. Assoc., 60, 1388-1399, 2010.
Lewandowski, M., Jaoui, M., Offenberg, J. H., Kleindienst, T. E., Edney, E. O., Sheesley, R. J., and Schauer, J. J.: Primary and secondary contributions to ambient $PM_{2.5}$ in the midwestern United States, Environ. Sci. Technol., 42, 3303-3309, 2008.

15. Page 7142 line 18: replace “emission and tracers partitioning.” With “emission and gas-particle partitioning.”
Reply: Replaced (Line 36 in the revised manuscript)

16. Page 7142, line 28: revise to “to estimate secondary”
Reply: Revised (Line 46 in the revised manuscript)

17. Page 7155, line 17 “not measure OC”
Reply: Revised (Line 440 in the revised manuscript)

18. Table 1 – improve the “Month column” The six numbers are not easily interpreted.
Suggest writing out the month and year, e.g. July 2012
Reply: Revised as suggested (Page 33 in the revised manuscript)

19. Figure 2 – suggest replacing numerical dates on the x-axis with “July 2012” to improve readability.
Reply: Revised as suggested. (Page 24 in the revised manuscript)

20. Table 1 – Indicate that temp and RH are monthly averages.
Reply: We indicated that “temperature and RH are monthly averages” as the note of Table 1. (Page 33 in the revised manuscript)

Works Cited

Duo, B., Y. Zhang, L. Kong, H. Fu, Y. Hu, J. Chen, L. Li and A. Qiong, 2015. Individual particle analysis of aerosols collected at Lhasa City in the Tibetan Plateau. Journal of Environmental Sciences-China 29, 165-177.
Eddingsaas, N. C., C. L. Loza, L. D. Yee, M. Chan, K. A. Schilling, P. S. Chhabra, J. H. Seinfeld and P. O. Wennberg, 2012. alpha-pinene photooxidation under controlled chemical conditions - Part 2: SOA yield and composition in low- and high-NOx environments. Atmospheric Chemistry and Physics 12 (16), 7413-7427.
Glasius, M., M. Lahaniati, A. Calogirou, D. Di Bella, N. R. Jensen, J. Hjorth, D. Kotzias and

B. R. Larsen, 2000. Carboxylic acids in secondary aerosols from oxidation of cyclic monoterpenes by ozone. Environmental Science & Technology 34 (6), 1001-1010.
Jaoui, M., T. E. Kleindienst, M. Lewandowski, J. H. Offenberg and E. O. Edney, 2005. Identification and quantification of aerosol polar oxygenated compounds bearing carboxylic or hydroxyl groups. 2. Organic tracer compounds from monoterpenes. Environmental Science & Technology 39 (15), 5661-5673.
Kleindienst, T. E., T. S. Conver, C. D. McIver and E. O. Edney, 2004. Determination of secondary organic aerosol products from the photooxidation of toluene and their implications in ambient PM2.5. Journal of Atmospheric Chemistry 47 (1), 79-100.
Kleindienst, T. E., M. Jaoui, M. Lewandowski, J. H. Offenberg, C. W. Lewis, P. V. Bhave and E. O. Edney, 2007. Estimates of the contributions of biogenic and anthropogenic hydrocarbons to secondary organic aerosol at a southeastern US location. Atmospheric Environment 41 (37), 8288-8300.
Lewis, A. C., M. J. Evans, J. R. Hopkins, S. Punjabi, K. A. Read, R. M. Purvis, S. J. Andrews, S. J. Moller, L. J. Carpenter, J. D. Lee, A. R. Rickard, P. I. Palmer and M. Parrington, 2013. The influence of biomass burning on the global distribution of selected non-methane organic compounds. Atmospheric Chemistry and Physics 13 (2), 851-867.
Meng, J., G. Wang, J. Li, C. Cheng and J. Cao, 2013. Atmospheric oxalic acid and related secondary organic aerosols in Qinghai Lake, a continental background site in Tibet Plateau. Atmospheric Environment 79, 582-589.
Stone, E. A., G. C. Lough, J. J. Schauer, P. S. Praveen, C. E. Corrigan and V. Ramanathan, 2007. Understanding the origin of black carbon in the atmospheric brown cloud over the Indian Ocean. Journal of Geophysical Research-Atmospheres 112 (D22).
Stone, E. A., T. T. Nguyen, B. B. Pradhan and P. M. Dangol, 2012. Assessment of biogenic secondary organic aerosol in the Himalayas. Environmental Chemistry 9, 263-272.
Szmigielski, R., J. D. Surratt, Y. Gomez-Gonzalez, P. Van der Veken, I. Kourtchev, R. Vermeylen, F. Blockhuys, M. Jaoui, T. E. Kleindienst, M. Lewandowski, J. H. Offenberg, E. O. Edney, J. H. Seinfeld, W. Maenhaut and M. Claeys, 2007. 3-methyl-1,2,3-butanetricarboxylic acid: An atmospheric tracer for terpene secondary organic aerosol. Geophysical Research Letters 34 (24).
Xiao, Q., E. Saikawa, R. J. Yokelson, P. Chen, C. Li and S. Kang, 2015. Indoor air pollution from burning yak dung as a household fuel in Tibet. Atmospheric Environment 102, 406-412.

Seasonal variation of secondary organic aerosol tracers in Central Tibetan Plateau

Ru-Qin Shen [a,c], Xiang Ding [a,*], Quan-Fu He [a,c], Zhi-Yuan Cong [b], Qing-Qing Yu [a,c], Xin-Ming Wang [a]

[a] State Key Laboratory of Organic Geochemistry, Guangzhou Institute of Geochemistry, Chinese Academy of Sciences, Guangzhou 510640, China

[b] Key Laboratory of Tibetan Environment Changes and Land Surface Processes, Institute of Tibetan Plateau Research, Chinese Academy of Sciences, Beijing 100085, China

[c] University of Chinese Academy of Sciences, Beijing, 100049, China

* Corresponding author

Dr. Xiang Ding

State Key Laboratory of Organic Geochemistry

Guangzhou Institute of Geochemistry, Chinese Academy of Sciences

511 Kehua Road, Guangzhou 510640, China

Tel: +86-20-85290127; Fax: +86-20-85290706

E-mail: xiangd@gig.ac.cn

Formatted

Deleted: Nam Co,

Formatted: Default Paragraph Font, Font: 小五

Abstract

Secondary organic aerosol (SOA) affects the earth's radiation balance and global climate. High-elevation areas are sensitive to global climate change. However, at present, SOA origins and seasonal variations are understudied in remote high-elevation areas. In this study, particulate samples were collected from July 2012 to July 2013 at the remote Nam Co (NC) site, Central Tibetan Plateau and analyzed for SOA tracers from biogenic (isoprene, monoterpenes and β-caryophyllene) and anthropogenic (aromatics) precursors. Among these compounds, isoprene SOA (SOA_I) tracers represented the majority (26.6 ± 44.2 ng m^{-3}), followed by monoterpene SOA (SOA_M) tracers (0.97 ± 0.57 ng m^{-3}), aromatic SOA (SOA_A) tracer (2,3-dihydroxy-4-oxopentanoic acid, DHOPA, 0.25 ± 0.18 ng m^{-3}) and β-caryophyllene SOA tracer (β-caryophyllenic acid, 0.09 ± 0.10 ng m^{-3}). SOA_I tracers exhibited high concentrations in the summer and low levels in the winter. The similar temperature dependence of SOA_I tracers and isoprene emission suggested that the seasonal variation of SOA_I tracers at the NC site was mainly influenced by the isoprene emission. The ratio of high-NOx to low-NOx products of SOA_I (2-methylglyceric acid to 2-methyltetrols) was the highest in the winter and the lowest in the summer, due to the influence of temperature and relative humidity. The seasonal variation of SOA_M tracers was impacted by monoterpenes emission and gas-particle partitioning. During the summer to the fall, temperature effect on partitioning was the dominant process influencing SOA_M tracers' variation; while the temperature effect on emission was the dominant process influencing SOA_M tracers' variation during the winter to the spring. SOA_M tracer levels did not elevate with increased temperature in the summer, probably resulting from the counteraction of temperature effects on emission and partitioning. The concentrations of DHOPA were 1-2 orders of magnitude lower than those reported in the urban regions of the world. Due to the transport of air pollutants from the adjacent Bangladesh and the northeastern India, DHOPA presented relatively higher levels in the summer. In the winter when air masses mainly came from the northwestern India, mass fractions of DHOPA in total tracers increased, although its concentrations declined. The SOA-tracer method was applied to estimate secondary organic carbon (SOC) from these four precursors. The annual average of SOC was 0.22 ± 0.29 μgC m^{-3}, with the biogenic SOC (sum of isoprene, monoterpenes and β-caryophyllene) accounting for 75%. In the summer, isoprene was the major precursor with its SOC contributions of 81%. In the winter when the emission of biogenic precursors largely dropped, the contributions of aromatic SOC increased. Our study implies that anthropogenic pollutants emitted in

Deleted: isoprene

Deleted: tracers

Formatted: Subscript

Formatted: Subscript

Deleted: The similar temperature dependence of SOAM tracers and monoterpenes emission was only observed

Deleted: gas/particle

Deleted: and monoterpenes emission

Formatted: Font: 10 pt

Deleted: d

the Indian subcontinent could transport to the TP and have impact on SOC over the remote NC.

Keywords: Secondary organic aerosol, Tibetan Plateau, Isoprene, Monoterpenes, Aromatics

1. Introduction

Organic aerosol affects the earth's radiation balance and global climate. As a large fraction of organic aerosol, secondary organic aerosol (SOA) is produced by homogenous (Claeys *et al.* 2004) and heterogeneous (Jang *et al.* 2002) reactions of volatile organic compounds (VOCs) as well as aging of organic aerosol (Robinson *et al.* 2007, Donahue *et al.* 2012). The global emission of biogenic VOCs (BVOCs), such as isoprene and monoterpenes (Guenther *et al.* 1995) were estimated to be one order of magnitude higher than those of anthropogenic sources (Piccot *et al.* 1992). Thus, global SOA is believed to be largely from BVOCs.

SOA tracers from specific VOCs can provide insight on processes and sources influencing SOA formation and spatiotemporal distribution. The identification of the isoprene SOA (SOA_I) tracers, 2-methyltetrols (Claeys *et al.* 2004) revealed the importance of SOA_I in global SOA burden. The further studies in high-NOx and low-NOx products of isoprene intermediates (e.g. methacrylic acid epoxide and isoprene epoxydiols) provided more details in the mechanisms of SOA_I formation under the influence of NOx (Paulot *et al.* 2009, Froyd *et al.* 2010, Surratt *et al.* 2010, Lin *et al.* 2013). The identification of tracers from aromatic SOA (SOA_A) (Offenberg *et al.* 2007) offered a way to directly evaluate the variation of anthropogenic SOA, particularly in urban regions. In addition, specific tracers have been determined in monoterpene SOA (SOA_M) (Jaoui *et al.* 2005, Claeys *et al.* 2007) and β-caryophyllene SOA (SOA_C) (Jaoui *et al.* 2007, van Eijck *et al.* 2013). Based on these SOA tracers, Kleindienst and coworkers further developed an SOA-tracer method to attribute SOA sources in the ambient air. Since it is difficult to directly measure SOA, the SOA-tracer method provides a valuable technique to estimate SOA in the ambient air, and it has been widely used around the world (Hu *et al.* 2008, von Schneidemesser *et al.* 2009, Guo *et al.* 2012, Lewandowski *et al.* 2013, Ding *et al.* 2014).

High-elevation areas are sensitive to global climate change (Xua *et al.* 2009). Observation of aerosol concentrations and compositions at high elevation sites can provide insight into the influence of natural and anthropogenic aerosols on global climate. The Tibetan Plateau (TP), the largest and highest plateau, is at the juncture of large desert areas and the densely populated Indian subcontinent. Previous

study found the northwesterly winds could bring dust from the western deserts to the TP and lead to high levels of geological aerosols at a site on the southeast TP (Zhao *et al.* 2013). Moreover, anthropogenic pollutants (e.g. sulfate, nitrate, potassium, element carbon, and heavy metals) emitted in the developing countries in South Asia could be transported to the TP by the southerly and southwesterly winds, especially during the summer monsoon season (Cong *et al.* 2007, Ming *et al.* 2010, Li *et al*. 2013, Zhao *et al.* 2013).

The observation at the remote central TP site, Nam Co (NC) discovered that the mean ratio of organic carbon (OC) to element carbon (EC) was 31.9 ± 31.1 during July 2006 to January 2007, implying the significant SOA contribution to OC (Ming *et al.* 2010) in the TP. However, there are only three studies in SOA compositions within the TP. Li et al. (2013) reported biogenic SOA (BSOA) tracers during the summer of 2010 at Qinghai Lake in the northeastern part of the TP. Stone et al., (2012) measured BSOA tracers from August to October 2005 on the south slope of Himalayas in the southwestern part of the TP. Due to the limited samples, it was difficult to examine the seasonal variation of these BSOA tracers in the TP. Moreover, due to the lack of anthropogenic SOA tracers, it was not possible to examine anthropogenic SOA in the TP, although above discussions have demonstrated that air pollutants from South Asia could be transported to the TP. Our recent study provided a snapshot of SOA tracers over China (including the NC and Linzhi sites in the TP) during the summer of 2012 (Ding *et al.* 2014). In this study, the observation at the remote NC site extended to one year. Seasonal trends of SOA tracers from isoprene, monoterpene, β-caryophyllene and aromatics were determined in the TP. Furthermore, secondary organic carbon (SOC) was estimated by the SOA-tracer method to check the variations of SOA origins at the NC site. To our knowledge, it is the first time that the seasonal trends of SOA tracers and origins are studied in the remote TP.

Deleted: its

2. Experiment

2.1 Field Sampling

Samples were collected at a remote site (4730 meters above sea level) at the southeastern shore of Nam Co Lake in the central TP (Figure 1). Nam Co Lake (90°16′ – 91°03′ E and 30°30′ – 30°55′N) is located in the Nyainqen Tanglha Mountain Range with a total area of 2017 km^2 (Zhou *et al.* 2013). The major vegetation in the Nam Co Lake Basin is the high cold alpine meadow.

Sampling was undertaken from July 2012 to July 2013. An Anderson sampler equipped with

9-stage cascade impactors and pre-baked quartz fiber filters (Whatman, baked at 450 ℃ for 8 h) was used to get size-segregated particle samples at an air flow rate of 28.3 L min^{-1}. The 50% cutoff sizes are <0.4, 0.4−0.7, 0.7−1.1, 1.1−2.1, 2.1−3.3, 3.3−4.7, 4.7−5.8, 5.8−9.0, and ⩾9.0 μm, respectively. The flow rate was calibrated before and after each sampling episode using an airflow meter to ensure the sampler operated at the specified flow rate. One set of 9 size-fractionated filters were collected for 72 hours every two weeks. Additionally, four sets of field blanks were collected in the same way as the ambient samples for 5 minutes when the sampler was turned off. All samples were wrapped with aluminum foil and stored at -18 ℃ before analysis.

2.2 Chemical Analysis

Each set of nine filters were combined together as one sample to meet the analysis requirement. Detailed information on the SOA tracer analysis is described elsewhere (Ding *et al.* 2014). Prior to solvent extraction, isotope-labeled standard mixtures were spiked into samples as internal standards. Samples were extracted twice by sonication with the mixed solvent dichloride methane (DCM)/hexane (1:1, v/v), then three times with the mixed solvent DCM/methanol (1:1, v/v). The extracts of each sample were combined, filtered and concentrated to ~2 mL. Then, the concentrated solution was divided into two parts for methylation and silylation, respectively.

The samples were analyzed by an a gas chromatography/mass spectrometer detector (GC/MSD, Agilent 7890/5975C) in the selected ion monitoring (SIM) mode with a 30 m HP-5 MS capillary column (i.d. 0.25 mm, 0.25 μm film thickness). Splitless injection of a 2 μL sample was performed. The GC temperature was initiated at 65 ℃, held for 2 min, then increased to 290 ℃ at 5 ℃ min^{-1} and held for 20 min. Thirteen SOA tracers were quantified by the GC/MSD coupled with an electron impact (EI) ionization source, including five SOA_M tracers (*cis*-pinonic acid, pinic acid, 3-methyl-1,2,3-butanetricarboxylic acid, 3-hydroxyglutaric acid and 3-hydroxy-4,4-dimethylglutaric acid), six SOA_I tracers (2-methylthreitol, 2-methylerythritol, 2-methylglyceric acid, *cis*-2-methyl-1,3,4-trihydroxy-1-butene, *trans*-2-methyl-1,3,4-trihydroxy-1-butene and 3-methyl-2,3,4-trihydroxy-1-butene), one SOA_C tracer (β-caryophyllenic acid) and one SOA_A tracer (2,3-dihydroxy-4-oxopentanoic acid, DHOPA). Figure S1 in supplemental information presents the total ion chromatogram (TIC) of these SOA tracers. *cis*-Pinonic acid and pinic acid were quantified by authentic standards. Due to the lack of standards, the SOA_I tracers were quantified using erythritol

Formatted: Font: Italic

Formatted: Font: Italic

Formatted: Font: Italic

Formatted: Font: Italic

(Claeys *et al.* 2004, Ding *et al.* 2008). The other SOA_M tracers were quantified using *cis*-pinonic acid. β-Caryophyllenic acid and DHOPA were quantified using octadecanoic acid and azelaic acid, respectively (Ding *et al.* 2012). The EI spectrum of each SOA tracer is shown in Figure S2-S4. The method detection limits (MDLs) for *cis*-pinonic acid, pinic acid, erythritol, octadecanoic acid and azelaic acid were 0.03, 0.05, 0.04, 0.03 and 0.07 ng m^{-3}, respectively, at a total volume of 122 m^3.

2.3 Quality assurance and quality control

Field and laboratory blanks were analyzed in the same manner as the field samples. These SOA tracers were not detected in the field or laboratory blanks. To evaluate the recoveries of the analytical method, six spiked samples (authentic standards spiked into solvent with pre-baked quartz filters) were analyzed. The recoveries were 101 ± 3 % for *cis*-pinonic acid, 70 ± 10 % for pinic acid, 65 ± 14 % for erythritol, 83 ± 7 % for octadecanoic acid, and 89 ± 9 % for azelaic acid. The relative differences for target compounds in samples collected in parallel (n=6) were all below 15%.

It should be noted that ketopinic acid was used as the surrogate for the quantification of all SOA tracers by Kleindienst et al. (2007); while different surrogates were used to quantify different SOA tracers in this study. The response factors of internal standard calibration for the 5 surrogates ranged from 0.98 (azelaic acid) to 1.78 (pinic acid), with the average of 1.38 and the relative standard deviation (RSD) of 23%. The response factor of ketopinic acid was also calculated in this study. Its value (1.27) was consistent with the average of the five surrogates.

2.4 Estimation of measurement uncertainty

Since there is no commercial standard available for most SOA tracers (except *cis*-pinonic acid and pinic acid), the use of surrogate standards for quantification introduces additional error to measurement. Error in analyte measurement (E_A) is propagated from the standard deviation of the field blank (E_{FB}), error in spike recovery (E_R) and the error from surrogate quantification (E_Q):

$$E_A = \sqrt{{E_{FB}}^2 + {E_R}^2 + {E_Q}^2} \quad (1)$$

Since SOA tracers were not detected in the field blanks, E_{FB} was 0 in this study. The spike recoveries of surrogate standards were used to estimate the E_R of tracers which ranged from 1% (*cis*-pinonic acid) to 35% (erythritol). Stone et al., (2012) developed an empirical approach to estimate E_Q based on homologous series of atmospherically relevant compounds. The relative error introduced

Formatted: Font: Italic

Formatted: Font: Italic

Formatted: Heading 1, Justified, Indent: First line: 0 ch, Space Before: 6 pt, Pattern: Clear (White)

Formatted: Font: Italic

Deleted: Thus, the quantification uncertainty caused by using surrogate calibration should be within 23%.

Deleted: was

Deleted: , which

Deleted: 2.3

Formatted: Normal, Left, Indent: First line: 0.74 cm, Space Before: 0 pt, Pattern: Clear

Formatted: Subscript

Formatted: Subscript

Formatted: Font: Italic

by each carbon atom (E_n) was estimated to be 15 %, each oxygenated functional group (E_f) to be 10% and alkenes (E_d) to be 60%. The errors introduced from surrogate quantification are treated as additive and are calculated as:

$$E_Q = E_n \Delta n + E_f \Delta f + E_d \Delta d \quad (2)$$

where Δn is the difference in carbon atom number between a surrogate and an analyte, Δf is the difference in oxygen-containing functional group between a surrogate and an analyte, Δd is the difference in alkene functionality between a surrogate and an analyte.

Table S1 shows the estimated uncertainties in tracer measurement. The errors from surrogate quantification (E_Q) ranged from 15% (2-methyltetrols) to 155% (β-caryophyllenic acid) in this study. Propagated with the error in recovery, the uncertainties in analyte measurement (E_A) were estimated in the range of 38% to 156%.

2.5 Backward trajectories

The air masses' transport during each sampling episode was investigated using Hybrid Single Particle Lagrangian Integrated Trajectory Model (HYSPLIT V4.9). Five-day backward trajectories (BTs) were analyzed during each sampling episode with 6-hour step at the height of 500 m above ground level. Then cluster analysis was performed to present the mean trajectory of each cluster, based on all the trajectories during our campaign.

3. Results and Discussions

3.1 Seasonal variations of SOA tracers

Since the NC site is located in the high elevation TP, the annual temperature was only -1.64 ℃ with the range of -16.1 ℃ in January to 10.2 ℃ in July (Table 1). The annual relative humidity (RH) was 58% with the peak in July (84%) and the lowest in January (30%). The sum of all tracers ranged from 0.78 to 185 ng m^{-3}. Among these compounds, SOA_I tracers (26.6 ± 44.2 ng m^{-3}) represented the majority, followed by SOA_M tracers (0.97 ± 0.57 ng m^{-3}), DHOPA (0.25 ± 0.18 ng m^{-3}) and β-caryophyllenic acid (0.09 ± 0.10 ng m^{-3}). During the summer (July-September 2012 and June-July 2013), SOA_I tracers presented the majority (> 95%). The mass fractions of SOA_M tracers in all compounds increased during the cold period (October 2012 to May 2013).

Formatted: Subscript
Formatted: Subscript
Formatted: Subscript
Formatted: Font: (Default) Times New Roman, (Asian) 宋体
Formatted: Font: (Default) Times New Roman, (Asian) 宋体
Formatted: Font: (Default) Times New Roman, (Asian) 宋体
Deleted: Quality assurance and quality control
Deleted: 2.4

3.1.1 Isoprene SOA tracers

The total concentrations of SOA_I tracers (sum of six tracers) ranged from 0.36 – 184 ng m^{-3}. The levels of SOA_I tracers were 1-2 orders of magnitude higher than those over the global oceans and the Arctic (Table 2). Among the SOA_I traces, 2-methyltetrols (sum of 2-methylthreitol and 2-methylerythritol, MTLs) were the major components (72%), with an annual average of 23.8 ± 40.3 ng m^{-3} (0.18 to 165 ng m^{-3}). The 2-methylglyceric acid (MGA) averaged 1.95 ± 2.92 ng m^{-3} and C_5-alkenetriols (sum of *cis*-2-methyl-1,3,4-trihydroxy-1-butene, *trans*-2-methyl-1,3,4-trihydroxy-1-butene, and 3-methyl-2,3,4-trihydroxy-1-butene) averaged 0.93 ± 1.39 ng m^{-3}. MTLs are produced through the particle-phase uptake of the epoxydiols that formed in the gas-phase photo-oxidation of isoprene under low-NOx or NOx free conditions (Paulot *et al.* 2009, Surratt *et al.* 2010). Since the remote TP is a low-NOx environment, it is expected that the low-NOx products, MTLs dominated over other SOA_I tracers. The majority of MTLs at the NC site was consistent with those observed within the TP (Stone *et al.* 2012, Li *et al.* 2013) and over most global oceans (Fu *et al.* 2011, Hu *et al.* 2013), but different from those over the North Pacific Ocean and the Arctic where MGA was the major SOA_I tracer due to the significant influence of Siberian fires (Fu *et al.* 2011, Ding *et al.* 2013). The two MTL isomers exhibited a strong correlation with each other throughout the year (R^2=0.996, p<0.001) with a slope of 3.7, indicating that the two isomers shared similar formation pathways.

Figure 2a presents a typical seasonal trend of SOA_I tracers that high concentrations all existed in the summer. From October 2012 to April 2013, temperature was below zero, the levels of SOA_I tracers dramatically decreased as low as 0.38 ng m^{-3} in January.

Isoprene emission rate (E_I) depends on light and temperature (Guenther *et al.* 1993):

$$E_I = EF_I \times C_L \times C_T \quad (3)$$

where EF_I is the basal emission rate at 30 °C leaf temperature and 1000 μmol m^{-2} s^{-1} PAR. C_L and C_T are the factors representing the influences of light and temperature, respectively. C_T can be estimated as:

$$C_T = \frac{exp^{\frac{C_{T1}(T-T_S)}{RT_ST}}}{1+exp^{\frac{C_{T2}(T-Tm)}{RT_ST}}} \quad (4)$$

Then the natural logarithm of C_T is calculated as:

Formatted: Font: Italic

Formatted: Font: Italic

Moved down [2]: The natural logarithm of SOA_I tracer levels exhibited a negative correlation with the reciprocal of temperature in Kelvin (p<0.01, Figure 3a).

Deleted: 1

Deleted: 2

$$\text{Ln } C_T = \frac{C_{T1}}{RT_s}\left(1 - \frac{T_s}{T}\right) - \text{Ln}[1 + exp^{\frac{C_{T2}}{RT_s}\left(1 - \frac{Tm}{T}\right)}] \quad (5)$$

where R = 8.314 J K^{-1} mol^{-1}, C_{T1} = 95000 J mol^{-1}, C_{T2} = 230000 J mol^{-1}, T_s = 303 K, T_m = 314 K, and T is the leaf temperature (Guenther *et al.* 1993). Under the condition of T < T_m, the latter part in Equation (5) is close to zero, and Ln C_T is linearly correlated with 1/T.

Figure 3a presents a negative correlation between the natural logarithm of SOA_I tracer levels and the reciprocal of temperature in Kelvin ($p<0.001$). Moreover, the temperature dependence of SOA_I tracers was similar to that of C_T, and SOA_I tracers exhibited a significant positive correlation with C_T during our sampling at the NC site (Figure 3b). These results indicated that the seasonal variation of SOA_I tracers at the NC site was mainly influenced by the isoprene emission. Considering the short lifetime (several hours) of isoprene in the air, SOA_I should be mainly formed from local precursor. In summer, high temperature and intense light could enhance isoprene emission and photo-reactions. Moreover, high temperature in summer could enhance the heterogeneous reactions of isoprene-derived epoxides on particles which play the key roles in SOA_I formation (Lin et al., 2013; Paulot et al., 2009). All these interpreted the high levels of SOA_I tracers in the summer at the NC site. In the winter, isoprene emission significantly dropped due to the extremely low temperature. Thus, the tracers were only in trace amount at the NC site.

It is worth noting that the ratio of MGA to MTLs (MGA/MTLs) was negatively correlated with temperature (Figure 4a) and RH (Figure 4b). Based on chamber results, the formation mechanisms of MGA and MTLs are quite different. MGA is produced under high-NO_x conditions; while MTLs are mainly formed under low-NO_x or NO_x free conditions (Surratt *et al.* 2010). Moreover, low RH (15 – 40 %) could enhance the formation of MGA in the particulate phase but not of MTLs (Zhang *et al.* 2011). In addition, high particle acidity would favor the formation of MTLs instead of MGA (Surratt *et al.* 2007). Although there are few data available in the TP, the aerosols are expected to be neutral at the remote NC site. Thus, the influence of acidity on MGA/MTLs should be not significant. Isoprene emission is apparently high in summer due to high temperature and light intensity, which could enhance the ratio of isoprene to NOx and favor MTLs formation at the NC site. Moreover, high RH (~70%) in the summer (Table 1) could not favor MGA formation. Thus, MGA/MTLs exhibited the lowest values (less than 0.1) in the summer samples (Figure 4). In the winter, both temperature and RH dropped to the lowest of the whole year. Low temperature reduced isoprene emission and low RH

Deleted: 3

Deleted: 3

Moved (insertion) [2]

Deleted: T

Deleted: exhibited a negative correlation with

Formatted: Indent: First line: 1.42 ch

Deleted: , Figure 3a

Deleted: As shown in Figure 3a, there is a negative correlation between

Deleted: Ln C_T and

Deleted: 1/T

Deleted: within the temperature range

Deleted: (-16.7 to 10.2 ℃)

Deleted: The similar temperature dependence of SOA_I tracers and C_T

Formatted: Subscript

Deleted: the

Deleted:

Formatted: Subscript

Deleted: and

Deleted: favor SOA_I formation

Formatted: Subscript

favored MGA formation. Thus, MGA/MTLs increased up to 0.8 in the winter samples (Figure 4).

3.1.2 Terpene SOA tracers

The total concentrations of SOA_M tracers (sum of five tracers) ranged from 0.11 – 2.39 ng m^{-3}. The levels of the SOA_M tracers were consistent with those over the global oceans and the Arctic (Table 2). Among these traces, *cis*-pinonic acid was the major compound (54%), with an annual average of 0.49 ± 0.38 ng m^{-3}, followed by pinic acid (0.22 ± 0.32 ng m^{-3}), 3-methyl-1,2,3-butanetricarboxylic acid (0.18 ± 0.25 ng m^{-3}), 3-hydroxyglutaric acid (0.08 ± 0.06 ng m^{-3}) and 3-hydroxy-4,4-dimethylglutaric acid (below MDL in the most samples).

The monthly variation of SOA_M tracers did not fully follow that of temperature (Figure 2b). From July to November 2012 (period 1), temperature decreased to -15 ℃; while SOA_M tracer levels increased as high as 1.99 ng m^{-3}. After that, both temperature and SOA_M tracers dropped to the lowest values in January 2013, and increased concurrently till April 2013 (period 2). During May to July 2013 (period 3), SOA_M tracer levels exhibited slight variation, although temperature kept increasing.

The seasonal variation of SOA_M tracers could be influenced by monoterpenes emission and gas-particle partitioning. Monoterpenes emission rate (E_M) is often assumed to be solely dependent on temperature (Guenther *et al.* 1993):

$$E_M = EF_M \times \gamma_T \quad (6)$$

$$\gamma_T = exp^{\beta(T-T_s)} \quad (7)$$

where EF_M is monoterpenes emission rate at a standard temperature T_s (303 K), γ_T is the activity factor by temperature, β is an empirical coefficient usually taken to be 0.09 K^{-1} (Guenther *et al.* 1993), T is the leaf temperature.

SOA yield (Y) of precursors could be expressed using an empirical relationship based on gas-particle partitioning of two semi-volatile products (Odum et al., 1996):

$$Y = M_0 \sum_i^2 \frac{\alpha_i K_i}{1 + M_0 K_i} \quad (8)$$

where M_0 (μg m^{-3}) is the total concentration of absorbing organic material, α_i is the mass stoichiometric coefficients of the product i, K_i (m^3 μg^{-1}) is the temperature-dependent partitioning coefficient of the semi-volatile compound i. Assuming a constant activity coefficient and mean molecular weight, the partitioning coefficient, K_i (T) at a certain temperature (T) could be estimated as (Sheehan and

Formatted: Font: Italic
Deleted: /
Deleted: 4
Deleted: 5
Formatted: Indent: First line: 1.42 ch
Formatted: Font color: Text 1
Formatted: Font color: Text 1
Formatted: Font: 10 pt, Font color: Text 1
Formatted: Font: 10 pt, Font color: Text 1
Formatted: Font: 10 pt, Font color: Text 1
Formatted ...
Formatted: Font: 10 pt, Font color: Text 1
Formatted: Font: 10 pt, Font color: Text 1
Formatted: Font: 10 pt, Font color: Text 1
Formatted: Font: 10 pt, Font color: Text 1
Formatted: Font: 10 pt, Font color: Text 1
Formatted: Font: 10 pt, Font color: Text 1
Formatted: Font: 10 pt, Font color: Text 1
Formatted: Font: 10 pt, Font color: Text 1
Formatted: Font: 10 pt, Font color: Text 1
Formatted: Font: 10 pt, Font color: Text 1
Formatted: Font: 10 pt, Font color: Text 1
Formatted: Font: 10 pt, Font color: Text 1
Formatted: Font: 10 pt, Font color: Text 1
Formatted: Font: 10 pt, Font color: Text 1
Formatted: Font: 10 pt, Font color: Text 1
Formatted: Font color: Text 1
Formatted: Font color: Text 1
Formatted: Font color: Text 1, Subscript
Formatted: Font color: Text 1
Formatted: Superscript
Formatted: Font color: Text 1, Superscript
Formatted: Font color: Text 1
Formatted: Font color: Text 1
Formatted: Font color: Text 1, Subscript
Formatted: Font color: Text 1
Formatted: Font color: Text 1
Formatted: Font color: Text 1, Subscript
Formatted: Font color: Text 1
Formatted: Font color: Text 1, Superscript
Formatted: Font color: Text 1
Formatted: Font color: Text 1, Superscript
Formatted: Font color: Text 1
Formatted: Font color: Text 1
Formatted: Font color: Text 1, Subscript
Formatted: Font color: Text 1
Formatted: Font color: Text 1

Bowman, 2001):

$$K_i(T) = K_i^* \frac{T}{T^*} exp\left[\frac{H_i}{R}\left(\frac{1}{T^*} - \frac{1}{T}\right)\right] \quad (9)$$

where K_i^* is an experimentally determined partitioning coefficient at a reference temperature, T^*, H_i is the vaporization enthalpy, R is the gas constant. To model the temperature-dependent absorptive partitioning, three parameters, α_i, K_i, and H_i are required for each condensable product.

Table S2 lists all the parameters for two-product model of α-pinene SOA which were also used to estimate the temperature effect on SOA partitioning by Sheehan and Bowman (2001). The available data of OC at the NC site were reported in the range of 1.18 to 2.26 μgC m^{-3} during July 2006 to January 2007 with an average of 1.66 μgC m^{-3} (Ming et al., 2010). Thus, M_0 is calculated as 2.32 μg m^{-3} by the average OC multiplying 1.4. Figure S5 shows the temperature dependence of α-pinene emission rate (γ_T) and SOA yield within the temperature range at the NC site (-16.7 to 10.2 ℃). Obviously, decreasing temperature could reduce the emission but enhance the gas to particle partitioning and SOA yield.

From July to November 2012 (period 1), high values of SOA_M tracers and SOA yield existed under low temperature, and SOA_M tracers were positively correlated with SOA yield (r=0.647, p<0.05, Figure 5a). These suggested that the temperature effect on partitioning was the dominant process influencing SOA_M tracers' variation during the period 1. From December 2012 to April 2013 (period 2), high values of SOA_M tracers and activity factor (γ_T) existed under high temperature, and SOA_M tracers were positively correlated with γ_T (r=0.741, p<0.05, Figure 5b). These suggested that the temperature effect on emission was the dominant process influencing SOA_M tracers' variation during the period 2. The increase of SOA_M tracer concentrations during spring was also observed in the southeastern United States (Ding *et al.* 2008), resulting from the enhancement of monoterpenes emission in spring (Kim 2011). From May to July 2013 (period 3), SOA_M tracer concentrations were relative stable, and there was no correlation of SOA_M tracers with γ_T or SOA yield (p>0.05). These might result from the counteraction of temperature effects on emission and partitioning during the summer.

Previous study proposed that *cis*-pinonic acid and pinic acid (P) were the first-generation products of SOA_M and only formed under low-NOx conditions (Eddingsaas et al. 2012). The dominance of *cis*-pinonic acid and pinic acid among SOA_M tracers at the remote NC site indicated that SOA_M there was mainly formed under low-NOx conditions. Moreover, *cis*-pinonic acid and pinic acid could be

Formatted: Right, Allow text to wrap in the middle of a word
Formatted ...
Formatted ...
Formatted: Indent: First line: 1.42 ch
Formatted ...
Formatted ...
Moved (insertion) [1]
Formatted ...
Formatted ...

further photo-degraded to high-generation products, e.g. 3-methyl-1,2,3-butanetricarboxylic acid (M) (Glasius et al. 2000; Jaoui et al. 2005; Szmigielski, et al., 2007). And the ratio of *cis*-pinonic acid plus pinic acid to 3-methyl-1,2,3-butanetricarboxylic acid (P/M) could be applied to trace the aging of SOA_M (Ding et al., 2011; Gómez-González et al., 2012). In the fresh chamber produced α-pinene SOA samples, the ratios of P/M were reported in the range of 1.51 to 3.21 (Offenberg, et al., 2007). In this study, the ratio of P/M averaged 16.7 ± 20.9. Thus, SOA_M was generally fresh at the NC site and should be mainly formed from local precursors. Figure 6 presents a negative correlation between P/M and temperature (r=-0.560, p=0.008). Higher P/M ratios were observed in the fall and the winter, and lower P/M ratios occurred in the spring and the summer. Since temperature has positive influence on photo-reaction rates, the higher temperature during the summer could accelerate the photochemistry in the air and result in P to M conversion being more efficient. Thus, SOA_M in the summer was more aged than that in the winter.

The levels of SOA_C tracer, β-caryophyllenic acid were in the range of below MDL to 0.40 ng m^{-3}. As Figure 2c shows, the levels elevated from July to November 2012 and dropped to below MDL in December 2012. Then, the concentrations increased from January to March 2013 and decreased from April to June 2013. β-Caryophyllenic acid was positively correlated with SOA_M tracers (p=0.025), indicating that the seasonal variation of β-caryophyllenic acid was similar with that of the SOA_M tracers.

3.1.3 Aromatic SOA tracer

The levels of SOA_A tracer, DHOPA were in the range of below MDL to 0.61 ng m^{-3}. This anthropogenic tracer was not detected or reported in global remote areas (Table 2). Due to few human activity at the remote NC site, the highest concentration of DHOPA was 1-2 orders of magnitude lower than those (up to 52 ng m^{-3}) reported in the urban regions of United States (Lewandowski *et al.* 2013) and China (Ding *et al.* 2014). DHOPA exhibited the higher concentrations in the summer and the lower levels in the winter (Figure 2d).

Besides urban emissions from solvent and fossil fuel use, biomass burning is an important source of aromatics in many parts of the world (Lewis et al. 2013). The local dung or biomass burning (Duo et al. 2015; Xiao et al. 2015) may be potential sources of aromatics in the TP. Hence, DHOPA may come from the processing of biomass burning emission. Figure 7 exhibits the monthly variation of biomass

Formatted: Font: Italic

Formatted: Subscript

Formatted: Subscript

Deleted: Apparently, the natural logarithm of γ_T is positively correlated with temperature. On the contrary, increasing temperature would favor the evaporation of SOA_M tracers from particle phase to gas phase; and decreasing temperature would favor the condensation of these tracers from gas phase to particle phase (Saathoff *et al.* 2009). Thus, it is complicated that the influence of temperature on SOA_M tracer levels in particle phase. .

During the period 1, decreasing temperature could reduce monoterpenes emission and reactions. However, SOA_M tracer levels were increasing, probably due to the dominant influence of partitioning over emission. During the period 2, both SOA_M tracer levels and temperature were increasing. The natural logarithm of SOA_M tracer levels were positively correlated with temperature (Figure 3b), which was similar to that between Ln γ_T and temperature within the temperature range at the NC site (Figure 3b). The similar temperature dependence of SOA_M tracers and γ_T indicated that the significant increase of SOA_M from winter to spring at the NC site was mainly influenced by monoterpenes emission. The increase of SOA_M tracer concentrations during spring was also observed in the southeastern United States (Ding *et al.* 2008), resulting from the enhancement of monoterpenes emission in spring (Kim 2011). During the period 3, high temperature could enhance monoterpenes emission and tracers formation; while it could favor the evaporation of these tracers from particle phase into gas phase. Thus, the relative stable of SOA_M tracer concentrations during the period 3 might reflect the counteraction of temperature effects on monoterpenes emission/tracers formation and gas/particle ...

Moved up [1]: The increase of SOA_M tracer concentrations during spring was also observed in the southeastern United States (Ding *et al.* 2008), resulting from the enhancement of monoterpenes emission in spring (Kim 2011).

Deleted: significantly

Deleted: declined

Formatted: Font: (Default) Times New Roman, 10 pt

Formatted: Font: (Default) Times New Roman, 10 pt

Formatted: Font: (Default) Times New Roman, 10 pt

burning tracer, levoglucosan during our sampling. The concentrations of levoglucosan ranged from 0.82 ng m^{-3} (October 2012) to 4.55 ng m^{-3} (April 2013) with a mean of 1.87±1.14 ng m^{-3}. Apparently, the monthly variation trend of levoglucosan was quite different from that of DHOPA. And there was no correlation between DHOPA and levoglucosan ($p>0.05$) (Figure S6). These indicated that DHOPA was not mainly from the processing of biomass burning emission at the NC site. Since there was few anthropogenic source near the remote NC site, the SOA_A tracer should be not locally formed but mainly transported from upwind regions.

To check the potential source areas of anthropogenic emissions, the satellite data of population density (http://sedac.ciesin.columbia.edu/theme/population), aerosol optical thickness (AOT, http://neo.sci.gsfc.nasa.gov/), tropospheric NO_2 vertical column densities (VCD, http://avdc.gsfc.nasa.gov/), and surface CO (https://www2.acd.ucar.edu/mopitt) were analysis on the global scale. As shown in Figure S7a, the northern Indian subcontinent was the most populated region of the world, with a population density of more than 1000 persons per km^2. Moreover, the plots of global AOT, tropospheric NO_2 VCD, and surface CO (Figure S7, b-d) all illustrated that the northern Indian subcontinent, including Bangladesh, Nepal, the northeastern India, and the northwestern India was the global hotspots of these anthropogenic pollutants. Compared with the northern Indian subcontinent, the TP exhibited extremely low population density and low levels of AOT, surface CO, and NO_2 VCD (Figure 8, a-d). Besides these satellite data, a recent study at a site in the northwestern India (Indo-Gangetic plain) witnessed extremely high levels (up to 2065 ng m-3) of polycyclic aromatic hydrocarbons which were mainly formed from anthropogenic combustion processes (Dubey et al., 2015). All these demonstrated that there were high anthropogenic emissions in the northern India subcontinent.

The TP features a monsoon climate (Cong *et al.* 2007, Ming *et al.* 2010, Zhao *et al.* 2013). Figure 9a presents the average trajectory of each cluster during our sampling in the whole year. The air masses over the NC were primarily from Bangladesh, Nepal and the northeastern India (cluster 1, 32%), the northwestern India (Indo-Gangetic basin) (cluster 3–6, 55%), and the Taklimakan Desert (cluster 2, 13%) during the sampling period. In the summer, the prevailing southerly winds (cluster 1, Figure 9b) passed through the heavily polluted areas in the Bangladesh and the northeastern India, and could bring anthropogenic pollutants into the TP. Previous studies in the TP have witnessed the enrichment of anthropogenic metals (Cong *et al.* 2007) and the enhancement of carbonaceous aerosols (Ming *et al.*

Formatted: Font: (Default) Times New Roman, 10 pt, Superscript
Formatted: Font: (Default) Times New Roman, 10 pt
Formatted: Font: (Default) Times New Roman, 10 pt
Formatted: Font: (Default) Times New Roman, 10 pt
Deleted: is
Deleted: no
Formatted: Subscript
Formatted: Superscript
Formatted: Subscript
Formatted: Subscript
Deleted: 5a
Deleted: 5b
Deleted: urban
Deleted: air

2010, Zhao *et al.* 2013) under the influence of summer monsoon. Thus, the increase of DHOPA levels at the NC site in the summer was mainly due to the transport of air pollutants from the upwind Bangladesh and the northeastern India.

In the winter, the air masses over the NC site were mainly originated from the northwestern India (Indo-Gangetic basin) by the westerly winds (Figure 9b). Compared with the summer samples, the winter samples underwent the longer distance transport. Moreover, extremely low temperature in the winter could reduce DHOPA formation. Therefore, the levels of DHOPA were lower in the winter. It is worth noting that the mass fractions of DHOPA in all tracers significantly elevated in the winter (less than 2% in the summer but up to 10% in January, Figure 2d), although its levels reduced. As described in equation (3) and (6), temperature is an important factor controlling BVOCs emission. The drop of temperature from the summer (up to 10.2 ℃) to the winter (low to -16.7 ℃) at the NC site would lead to the emission of isoprene and monoterpenes decreasing by 98% and 90%, respectively. The elevated fractions of DHOPA in the winter samples suggested that the SOA contributions from aromatics would increase in the winter when BVOCs emission largely decreased.

3.2 Source apportionment

The SOA-tracer method developed by Kleindienst and co-workers was applied to attribute SOC at the NC site. The researchers performed chamber experiments to obtain the mass fraction of the tracers in SOC (f_{SOC}) for individual precursor:

$$f_{SOC} = \frac{\sum_i [tri]}{[SOC]} \quad (10)$$

where $\sum_i$[tri] is the total concentrations of the tracers for a certain precursor, [SOC] is the mass concentration of SOC. With these f_{SOC} values and the measured SOA tracers in the ambient air, SOC from different precursors can be estimated in the atmosphere, with the assumption that the f_{SOC} values in the chamber are the same as those in the ambient air. There is some degree of uncertainty in the SOA-tracer method due to the quantification with a single surrogate calibration standard (ketopinic acid) and the simplification of applying SOA tracers and conversion factors to calculate SOC in the ambient samples (Kleindienst *et al.* 2007). However, this method has been widely applied to attribute SOC from different precursors and proven to be able to provide reasonable results in the United States (Kleindienst *et al.* 2007, Stone *et al.* 2009, Lewandowski *et al.* 2013), and China (Hu *et al.* 2008, Guo

Deleted:
Deleted: 5b
Deleted: As c
Deleted: 1
Deleted: 4
Deleted: 6
Deleted: ;
Deleted: Kleindienst *et al.* 2010,
Deleted: 2012

et al. 2012, Peng *et al.* 2013, Ding *et al.* 2014). Lewandowski et al. (2008) found that the measured OC in the midwestern United States could be fully explained by primary OC from chemical mass balance (CMB) model plus SOC from the SOA-tracer method, suggesting that the secondary organic tracer technique could be a valuable method for SOC estimation. Kleindienst et al. (2010) further compared the estimated SOC by the SOA-tracer method and other four independent methods (multiple regressions, CMB, carbon isotope and EC-tracer) in the southeastern United States, and found that these five methods matched well. Our previous study in the Pearl River Delta found SOC levels estimated by the SOA-tracer method were not only consistent with but also correlated well with those by EC-tracer method in summer, (Ding et al., 2012). The SOC apportionment results were also comparable between the SOA-tracer method and positive matrix factorization (PMF) model in Hong Kong (Hu et al. 2010).

The f_{SOC} were reported as 0.155 ± 0.039 μg μgC^{-1}, 0.023 ± 0.0046 μg μgC^{-1} and 0.00797 ± 0.0026 μg μgC^{-1} for isoprene (SOC_I), β-caryophyllene (SOC_C) and aromatics (SOC_A), respectively (Kleindienst *et al.* 2007). In this study, the same set of SOA tracers as reported by Kleindienst et al. (2007) were used for SOC estimation, including MGA and MTLs for SOC_I, β-caryophyllenic acid for SOC_C and DHOPA for SOC_A. For monoterpene SOC (SOC_M), nine tracers were involved in the source profile (Kleindienst *et al.* 2007). However, only five of the nine SOA_M tracers were measured in the current study. Wang et al. (2013) compared the results from model prediction with field observation in the Pearl River Delta and pointed out that the SOA-tracer method would underestimate SOA_M, probably due to the mismatch of tracer compositions in the field and the source profile (Ding *et al.* 2014). To minimize the uncertainty caused by the mismatch in tracer compositions, the f_{SOC} with the same five SOA_M tracers (0.059 μg μgC^{-1}) was computed using the chamber data from another study by the same research group (Offenberg *et al.* 2007). The same f_{SOC} for SOA_M was also applied to estimate SOC_M in our previous study over China (Ding *et al.* 2014).

The uncertainty in the SOA-tracer method is induced from the analysis of organic tracers and the determination of the conversion factors. Based on the E_A values in Table S1, the uncertainties in the tracer analyses were within 40% for SOA_I (only MGA and MTLs involved for SOC estimation), 95% for SOA_M, 156% for SOA_C, and 91% for SOA_A. The uncertainties of f_{SOC} were reported to be 25% for isoprene, 48% for monoterpenes, 22% for β-caryophyllene and 33% for aromatics (Kleindienst *et al.* 2007, Lewandowski *et al.* 2013). Considering these factors, the uncertainties of SOC apportionment

Deleted: The

Deleted: 23

Deleted: in this study.

Formatted: Subscript

Formatted: Font color: Red

were calculated through error propagation. The RSD were 47% for SOC_I, 106% for SOC_M, 157% for SOC_C, and 96% for SOC_A. On average, the RSD of the reconstructed SOC (sum of the four precursors) was 51±11%.

Figure 10 presents the monthly variations of the reconstructed SOC. SOC was high in the summer 2012 and declined from October to December. After that, it kept increasing from January to June. The total concentrations of SOC ranged from 0.02 μgC m^{-3} to 0.69 μgC m^{-3} with an annual average of 0.22 ± 0.29 μgC m^{-3}. The available data of OC in total suspended particles at the NC site were reported in the range of 1.18 to 2.26 μgC m^{-3} during July 2006 to January 2007 (Ming *et al.* 2010). Since we did not measure OC in our size-segregated samples, the OC data reported by Ming et al. (2010) were used to calculate SOC fraction in OC (SOC/OC) from July to January. The calculated SOC/OC was average 38% in the summer and up to 58% in September, suggesting that SOC was an important contributor to OC at the NC site during the summer (Ming *et al.* 2010). However, from the fall to winter, the elevated OC and decreased SOC led to SOC/OC declining from 11% (in October) to 1% (in January), indicating that SOA from the four precursors had minor contributions to the elevated OC. Since the air masses during the fall to the winter were mostly originated from the northwestern Indo-Gangetic basin (cluster 3-6 in Figure 9), primary pollutants emitted there could transport to the TP and have significant impact on the air at the NC site. In addition, SOA from aqueous-phase reactions and primary OA aging could not be captured by the SOA-tracer method. Thus, the current results might underestimate the total amount of SOC, which partly explained the low OC shares of SOC at the NC site during the fall to the winter.

Biogenic SOC (sum of SOC_I, SOC_M, and SOC_C) dominated over SOC_A at the NC site, averagely accounting for 75% of the estimated SOC. In the summer, SOC_I was the major contributor with the SOC shares of 81%. From the fall to the spring, SOC_M became the major contributor, averagely contributing 38% to SOC. Although SOC_A level reduced in the winter, SOC_A contribution elevated as high as 53% in January 2013. The elevated OC and the higher SOC_A contribution in the winter samples (Figure 10) implied that the transport of anthropogenic pollutants from the Indian subcontinent might have significant influence on carbonaceous aerosols over the remote NC during winter.

4. Conclusion

Seasonal trends of SOA tracers and origins were studied in the remote TP for the first time. SOA_I

Deleted: 34
Deleted: 53
Deleted: 32
Deleted: 40
Deleted: 27
Formatted: Font: Times New Roman
Deleted: 6
Deleted: d
Deleted: during
Deleted: 5
Deleted: anthropogenic SOC (
Deleted:)
Deleted: 6
Deleted: its

tracers represented the majority among these compounds. The significant temperature dependence of SOA_I tracers suggested that the seasonal variation of SOA_I tracers at the NC site was mainly influenced by the isoprene emission. Due to the influence of temperature and relative humidity, the ratio of high-NOx to low-NOx products of SOA_I (MGA/MTLs) was the highest in the winter and the lowest in the summer. The seasonal variation of SOA_M tracers was impacted by monoterpenes emission and gas-particle partitioning. Due to the transport of air pollutants from the Indian subcontinent, DHOPA presented relatively higher concentrations in the summer and increased mass fractions in the winter. The SOA-tracer method was applied to estimated SOC from these four precursors. The annual average of SOC was 0.22 ± 0.29 μgC m^{-3}, with the biogenic SOC accounting for 75%. In the summer, isoprene was the major precursor with its SOC shares of 81%. In the winter when the emissions of biogenic precursors largely declined, the contributions of SOC_A increased. At present, SOA origins and their seasonal variations are unclear in the remote high-elevation TP. The remote TP is connected to the densely populated Indian subcontinent. Our study implies that anthropogenic pollutants emitted there could transport to the TP and influence SOC over the remote NC.

Deleted: isoprene

Deleted: tracers

Acknowledgment

This research was supported by the Strategic Priority Research Program of the Chinese Academy of Sciences (CAS) (XDA05100104/XDB05010200/XDA05100105), the National Science Foundation of China (41273116/41473099), and Youth Innovation Promotion Association, CAS.

References

Claeys, M., Graham, B., Vas, G., Wang, W., Vermeylen, R., Pashynska, V., Cafmeyer, J., Guyon, P., Andreae, M. O., Artaxo, P., and Maenhaut, W.: Formation of secondary organic aerosols through photooxidation of isoprene, Science, 303, 1173-1176, 2004.

Claeys, M., Szmigielski, R., Kourtchev, I., Van der Veken, P., Vermeylen, R., Maenhaut, W., Jaoui, M., Kleindienst, T. E., Lewandowski, M., Offenberg, J. H., and Edney, E. O.: Hydroxydicarboxylic acids: Markers for secondary organic aerosol from the photooxidation of alpha-pinene, Environ. Sci. Technol., 41, 1628-1634, 2007.

Cong, Z. Y., Kang, S. C., Liu, X. D., and Wang, G. F.: Elemental composition of aerosol in the Nam Co region, Tibetan Plateau, during summer monsoon season, Atmos. Environ., 41, 1180-1187, 2007.

Ding, X., Zheng, M., Yu, L. P., Zhang, X. L., Weber, R. J., Yan, B., Russell, A. G., Edgerton, E. S., and Wang, X. M.: Spatial and seasonal trends in biogenic secondary organic aerosol tracers and water-soluble organic carbon in the southeastern United States, Environ. Sci. Technol., 42, 5171-5176, 2008.

Ding, X., Wang, X., and Zheng, M.: The influence of temperature and aerosol acidity on biogenic secondary organic aerosol tracers: Observations at a rural site in the central Pearl River Delta region, South China, Atmos. Environ., 45, 1303-1311, 2011.

Ding, X., Wang, X. M., Gao, B., Fu, X. X., He, Q. F., Zhao, X. Y., Yu, J. Z., and Zheng, M.: Tracer-based estimation of secondary organic carbon in the Pearl River Delta, south China, J. Geophys. Res.-Atmos., 117, D05313, DOI: 10.1029/2011jd016596, 2012.

Ding, X., Wang, X. M., Xie, Z. Q., Zhang, Z., and Sun, L. G.: Impacts of Siberian biomass burning on organic aerosols over the North Pacific Ocean and the Arctic: Primary and secondary organic tracers, Environ. Sci. Technol., 47, 3149-3157, 2013.

Ding, X., He, Q.-F., Shen, R.-Q., Yu, Q.-Q., and Wang, X.-M.: Spatial distributions of secondary organic aerosols from isoprene, monoterpenes, β-caryophyllene, and aromatics over China during summer, J. Geophys. Res.-Atmos., 119, 11877-11891, 2014.

Donahue, N. M., Henry, K. M., Mentel, T. F., Kiendler-Scharr, A., Spindler, C., Bohn, B., Brauers, T., Dorn, H. P., Fuchs, H., Tillmann, R., Wahner, A., Saathoff, H., Naumann, K.-H., Moehler, O., Leisner, T., Mueller, L., Reinnig, M.-C., Hoffmann, T., Salo, K., Hallquist, M., Frosch, M., Bilde, M., Tritscher, T., Barmet, P., Praplan, A. P., DeCarlo, P. F., Dommen, J., Prevot, A. S. H., and Baltensperger, U.: Aging of biogenic secondary organic aerosol via gas-phase OH radical reactions, Proc. Natl. Acad. Sci. U. S. A., 109, 13503-13508, 2012.

Dubey, J., Maharaj Kumari, K., and Lakhani, A.: Chemical characteristics and mutagenic activity of PM2.5 at a site in the Indo-Gangetic plain, India, Ecotoxicol. Environ. Saf., 114, 75-83, 2015.

Duo, B., Zhang, Y., Kong, L., Fu, H., Hu, Y., Chen, J., Li, L., and Qiong, A.: Individual particle analysis of aerosols collected at Lhasa City in the Tibetan Plateau, J. Environ. Sci., 29, 165-177, 2015.

Eddingsaas, N. C., Loza, C. L., Yee, L. D., Chan, M., Schilling, K. A., Chhabra, P. S., Seinfeld, J. H., and Wennberg, P. O.: α-pinene photooxidation under controlled chemical conditions – Part 2: SOA yield and composition in low- and high-NOx environments, Atmos. Chem. Phys., 12, 7413-7427, 10.5194/acp-12-7413-2012, 2012.

Froyd, K. D., Murphy, S. M., Murphy, D. M., de Gouw, J. A., Eddingsaas, N. C., and Wennberg, P. O.: Contribution of isoprene-derived organosulfates to free tropospheric aerosol mass, Proc. Natl. Acad. Sci. U. S. A., 107, 21360-21365, 2010.

Fu, P. Q., Kawamura, K., Chen, J., and Barrie, L. A.: Isoprene, monoterpene, and sesquiterpene oxidation products in the high Arctic aerosols during late winter to early summer, Environ. Sci. Technol., 43, 4022-4028, 2009.

Formatted: Font: (Default) Times New Roman

Fu, P. Q., Kawamura, K., and Miura, K.: Molecular characterization of marine organic aerosols collected during a round-the-world cruise, J. Geophys. Res.-Atmos., 116, D13302, DOI: 10.1029/2011jd015604, 2011.

Fu, P. Q., Kawamura, K., Chen, J., Charrière, B., and Sempéré, R.: Organic molecular composition of marine aerosols over the Arctic Ocean in summer: contributions of primary emission and secondary aerosol formation, Biogeosciences, 10, 653-667, 2013.

Glasius, M., Lahaniati, M., Calogirou, A., Di Bella, D., Jensen, N. R., Hjorth, J., Kotzias, D., and Larsen, B. R.: Carboxylic acids in secondary aerosols from oxidation of cyclic monoterpenes by ozone, Environ. Sci. Technol., 34, 1001-1010, 2000.

Gómez-González, Y., Wang, W., Vermeylen, R., Chi, X., Neirynck, J., Janssens, I. A., Maenhaut, W., and Claeys, M.: Chemical characterisation of atmospheric aerosols during a 2007 summer field campaign at Brasschaat, Belgium: sources and source processes of biogenic secondary organic aerosol, Atmos. Chem. Phys., 12, 125-138, 2012.

Guenther, A., Hewitt, C. N., Erickson, D., Fall, R., Geron, C., Graedel, T., Harley, P., Klinger, L., Lerdau, M., Mckay, W. A., Pierce, T., Scholes, B., Steinbrecher, R., Tallamraju, R., Taylor, J., and Zimmerman, P.: A global-model of natural volatile organic-compound emissions, J. Geophys. Res.-Atmos., 100, 8873-8892, 1995.

Guenther, A. B., Zimmerman, P. R., Harley, P. C., Monson, R. K., and Fall, R.: Isoprene and monoterpene emission rate variability - Model evaluations and sensitivity analyses, J. Geophys. Res.-Atmos., 98, 12609-12617, 1993.

Guo, S., Hu, M., Guo, Q., Zhang, X., Zheng, M., Zheng, J., Chang, C. C., Schauer, J. J., and Zhang, R.: Primary sources and secondary formation of organic aerosols in Beijing, China, Environ. Sci. Technol., 46, 9846-9853, 2012.

Hu, D., Bian, Q., Li, T. W. Y., Lau, A. K. H., and Yu, J. Z.: Contributions of isoprene, monoterpenes, β-caryophyllene, and toluene to secondary organic aerosols in Hong Kong during the summer of 2006, J. Geophys. Res.-Atmos., 113, D22206, DOI: 10.1029/2008jd010437, 2008.

Hu, D., Bian, Q., Lau, A. K. H., and Yu, J. Z.: Source apportioning of primary and secondary organic carbon in summer $PM_{2.5}$ in Hong Kong using positive matrix factorization of secondary and primary organic tracer data, J. Geophys. Res.-Atmos., 115, D16204, doi: 10.1029/2009JD012498, 2010.

Hu, Q. H., Xie, Z. Q., Wang, X. M., Kang, H., He, Q. F., and Zhang, P.: Secondary organic aerosols over oceans via oxidation of isoprene and monoterpenes from Arctic to Antarctic, Sci. Rep., 3, 2280, 2013.

Jang, M. S., Czoschke, N. M., Lee, S., and Kamens, R. M.: Heterogeneous atmospheric aerosol production by acid-catalyzed particle-phase reactions, Science, 298, 814-817, 2002.

Jaoui, M., Kleindienst, T. E., Lewandowski, M., Offenberg, J. H., and Edney, E. O.: Identification and quantification of aerosol polar oxygenated compounds bearing carboxylic or hydroxyl groups. 2.

Formatted: Subscript

Organic tracer compounds from monoterpenes, Environ. Sci. Technol., 39, 5661-5673, 2005.

Jaoui, M., Lewandowski, M., Kleindienst, T. E., Offenberg, J. H., and Edney, E. O.: β-Caryophyllinic acid: An atmospheric tracer for β-caryophyllene secondary organic aerosol, Geophys. Res. Lett., 34, L05816, DOI: 10.1029/2006gl028827, 2007.

Kim, J.-C.: Factors controlling natural VOC emissions in a southeastern US pine forest, Atmos. Environ., 35, 3279-3292, 2001.

Kleindienst, T. E., Jaoui, M., Lewandowski, M., Offenberg, J. H., Lewis, C. W., Bhave, P. V., and Edney, E. O.: Estimates of the contributions of biogenic and anthropogenic hydrocarbons to secondary organic aerosol at a southeastern US location, Atmos. Environ., 41, 8288-8300, 2007.

Kleindienst, T. E., Lewandowski, M., Offenberg, J. H., Edney, E. O., Jaoui, M., Zheng, M., Ding, X., and Edgerton, E. S.: Contribution of primary and secondary sources to organic aerosol and PM2.5 at SEARCH network sites, J. Air Waste Manage. Assoc., 60, 1388-1399, 2010.

Lewandowski, M., Jaoui, M., Offenberg, J. H., Kleindienst, T. E., Edney, E. O., Sheesley, R. J., and Schauer, J. J.: Primary and secondary contributions to ambient $PM_{2.5}$ in the midwestern United States, Environ. Sci. Technol., 42, 3303-3309, 2008.

Lewandowski, M., Piletic, I. R., Kleindienst, T. E., Offenberg, J. H., Beaver, M. R., Jaoui, M., Docherty, K. S., and Edney, E. O.: Secondary organic aerosol characterisation at field sites across the United States during the spring-summer period, Int. J. Environ. Anal. Chem., 93, 1084-1103, 2013.

Lewis, A. C., Evans, M. J., Hopkins, J. R., Punjabi, S., Read, K. A., Purvis, R. M., Andrews, S. J., Moller, S. J., Carpenter, L. J., Lee, J. D., Rickard, A. R., Palmer, P. I., and Parrington, M.: The influence of biomass burning on the global distribution of selected non-methane organic compounds, Atmos. Chem. Phys., 13, 851-867, 2013.

Li, J. J., Wang, G. H., Wang, X. M., Cao, J. J., Sun, T., Cheng, C. L., Meng, J. J., Hu, T. F., and Liu, S. X.: Abundance, composition and source of atmospheric PM2.5 at a remote site in the Tibetan Plateau, China, Tellus Ser. B-Chem. Phys. Meteorol., 65, 20281, DOI:10.3402/tellusb.v65i0.20281, 2013.

Lin, Y. H., Zhang, H. F., Pye, H. O. T., Zhang, Z. F., Marth, W. J., Park, S., Arashiro, M., Cui, T. Q., Budisulistiorini, H., Sexton, K. G., Vizuete, W., Xie, Y., Luecken, D. J., Piletic, I. R., Edney, E. O., Bartolotti, L. J., Gold, A., and Surratt, J. D.: Epoxide as a precursor to secondary organic aerosol formation from isoprene photooxidation in the presence of nitrogen oxides, Proc. Natl. Acad. Sci. U. S. A., 110, 6718-6723, 2013.

Ming, J., Xiao, C. D., Sun, J. Y., Kang, S. C., and Bonasoni, P.: Carbonaceous particles in the atmosphere and precipitation of the Nam Co region, central Tibet, J. Environ. Sci., 22, 1748-1756, 2010.

Odum, J. R., Hoffmann, T., Bowman, F., Collins, D., Flagan, R. C., and Seinfeld, J. H.: Gas/particle partitioning and secondary organic aerosol yields, Environ. Sci. Technol., 30, 2580-2585, 1996.

Formatted: Subscript

Formatted: Font color: Auto

Offenberg, J. H., Lewis, C. W., Lewandowski, M., Jaoui, M., Kleindienst, T. E., and Edney, E. O.: Contributions of toluene and α-pinene to SOA formed in an irradiated toluene/α-pinene/NOx/ air mixture: Comparison of results using ^{14}C content and SOA organic tracer methods, Environ. Sci. Technol., 41, 3972-3976, 2007.

Paulot, F., Crounse, J. D., Kjaergaard, H. G., Kurten, A., St Clair, J. M., Seinfeld, J. H., and Wennberg, P. O.: Unexpected epoxide formation in the gas-phase photooxidation of isoprene, Science, 325, 730-733, 2009.

Peng, J. L., Li, M., Zhang, P., Gong, S. Y., Zhong, M. A., Wu, M. H., Zheng, M., Chen, C. H., Wang, H. L., and Lou, S. R.: Investigation of the sources and seasonal variations of secondary organic aerosols in PM2.5 in Shanghai with organic tracers, Atmos. Environ., 79, 614-622, 2013.

Piccot, S. D., Watson, J. J., and Jones, J. W.: A global inventory of volatile organic-compound emissions from anthropogenic sources, J. Geophys. Res.-Atmos., 97, 9897-9912, 1992.

Robinson, A. L., Donahue, N. M., Shrivastava, M. K., Weitkamp, E. A., Sage, A. M., Grieshop, A. P., Lane, T. E., Pierce, J. R., and Pandis, S. N.: Rethinking organic aerosols: Semivolatile emissions and photochemical aging, Science, 315, 1259-1262, 2007.

Sheehan, P. E., and Bowman, F. M.: Estimated effects of temperature on secondary organic aerosol concentrations, Environ. Sci. Technol., 35, 2129-2135, 2001.

Stone, E. A., Zhou, J., Snyder, D. C., Rutter, A. P., Mieritz, M., and Schauer, J. J.: A comparison of summertime secondary organic aerosol source contributions at contrasting urban locations, Environ. Sci. Technol., 43, 3448-3454, 2009.

Stone, E. A., Nguyen, T. T., Pradhan, B. B., and Dangol, P. M.: Assessment of biogenic secondary organic aerosol in the Himalayas, Environ. Chem., 9, 263-272, 2012.

Surratt, J. D., Lewandowski, M., Offenberg, J. H., Jaoui, M., Kleindienst, T. E., Edney, E. O., and Seinfeld, J. H.: Effect of acidity on secondary organic aerosol formation from isoprene, Environ. Sci. Technol., 41, 5363-5369, 2007.

Surratt, J. D., Chan, A. W. H., Eddingsaas, N. C., Chan, M. N., Loza, C. L., Kwan, A. J., Hersey, S. P., Flagan, R. C., Wennberg, P. O., and Seinfeld, J. H.: Reactive intermediates revealed in secondary organic aerosol formation from isoprene, Proc. Natl. Acad. Sci. U. S. A., 107, 6640-6645, 2010.

Szmigielski, R., Surratt, J. D., Gómez-González, Y., Veken, P. V. d., Kourtchev, I., Vermeylen, R., Blockhuys, F., Jaoui, M., Kleindienst, T. E., Lewandowski, M., Offenberg, J. H., Edney, E. O., Seinfeld, J. H., Maenhaut, W., and Claeys, M.: 3-Methyl-1,2,3-butanetricarboxylic acid: An atmospheric tracer for terpene secondary organic aerosol, Geophys. Res. Lett., 34, L24811, doi:10.1029/2007GL031338, 2007

van Eijck, A., Opatz, T., Taraborrelli, D., Sander, R., and Hoffmann, T.: New tracer compounds for secondary organic aerosol formation from beta-caryophyllene oxidation, Atmos. Environ., 80, 122-130, 2013.

Formatted: Superscript

Deleted: Epoxide

Deleted: Formation

Deleted: Gas

Deleted: Phase

Deleted: Photooxidation

Deleted: Isoprene

Deleted: Saathoff, H., Naumann, K. H., Mohler, O., Jonsson, A. M., Hallquist, M., Kiendler-Scharr, A., Mentel, T. F., Tillmann, R., and Schurath, U.: Temperature dependence of yields of secondary organic aerosols from the ozonolysis of alpha-pinene and limonene, Atmos. Chem. Phys., 9, 1551-1577, 2009.

von Schneidemesser, E., Schauer, J. J., Hagler, G. S. W., and Bergin, M. H.: Concentrations and sources of carbonaceous aerosol in the atmosphere of Summit, Greenland, Atmos. Environ., 43, 4155-4162, 2009.

Wang, S. Y., Wu, D. W., Wang, X. M., Fung, J. C. H., and Yu, J. Z.: Relative contributions of secondary organic aerosol formation from toluene, xylenes, isoprene, and monoterpenes in Hong Kong and Guangzhou in the Pearl River Delta, China: an emission-based box modeling study, J. Geophys. Res.-Atmos., 118, 507-519, 2013.

Xiao, Q., Saikawa, E., Yokelson, R. J., Chen, P., Li, C., and Kang, S.: Indoor air pollution from burning yak dung as a household fuel in Tibet, Atmos. Environ., 102, 406-412, 2015.

Xua, B., Cao, J., Hansen, J., Yao, T., Joswia, D. R., Wang, N., Wu, G., Wang, M., Zhao, H., Yang, W., Liu, X., and He, J.: Black soot and the survival of Tibetan glaciers, Proc. Natl. Acad. Sci. U. S. A., 106, 22114-22118, 2009.

Zhang, H., Surratt, J. D., Lin, Y. H., Bapat, J., and Kamens, R. M.: Effect of relative humidity on SOA formation from isoprene/NO photooxidation: enhancement of 2-methylglyceric acid and its corresponding oligoesters under dry conditions, Atmos. Chem. Phys., 11, 6411-6424, 2011.

Zhao, Z. Z., Cao, J. J., Shen, Z. X., Xu, B. Q., Zhu, C. S., Chen, L. W. A., Su, X. L., Liu, S. X., Han, Y. M., Wang, G. H., and Ho, K. F.: Aerosol particles at a high-altitude site on the Southeast Tibetan Plateau, China: Implications for pollution transport from South Asia, J. Geophys. Res.-Atmos., 118, 11360-11375, 2013.

Zhou, S. Q., Kang, S. C., Chen, F., and Joswiak, D. R.: Water balance observations reveal significant subsurface water seepage from Lake Nam Co, south-central Tibetan Plateau, J. Hydrol., 491, 89-99, 2013.

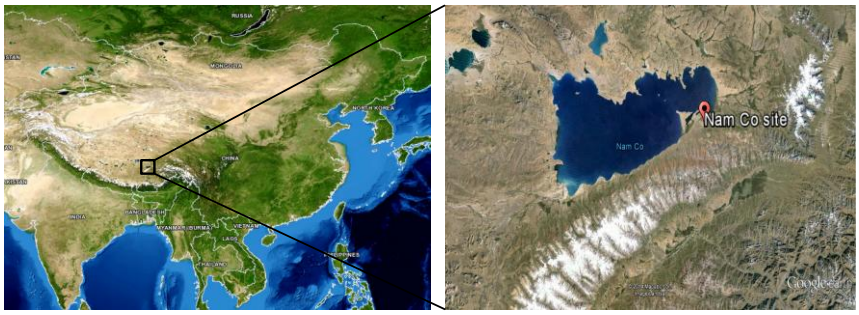

Figure 1 Nam Co site in the Tibetan Plateau, China

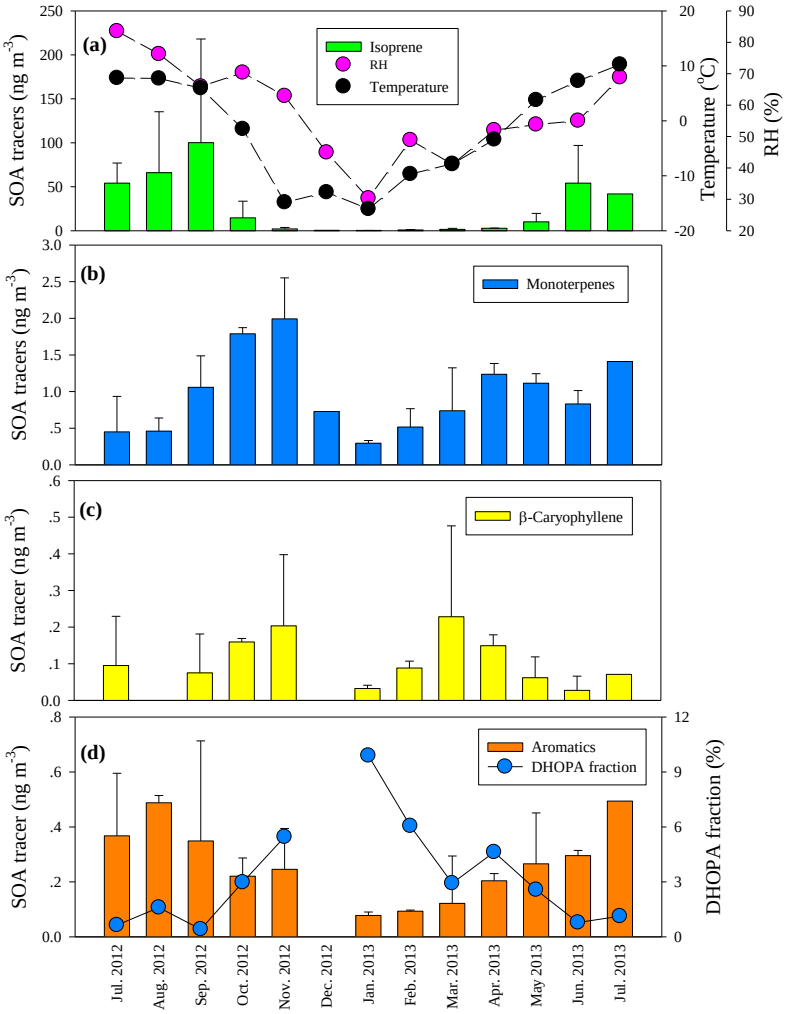

Figure 2 Monthly variations of SOA tracers.

Formatted: Font: (Default) Times New Roman

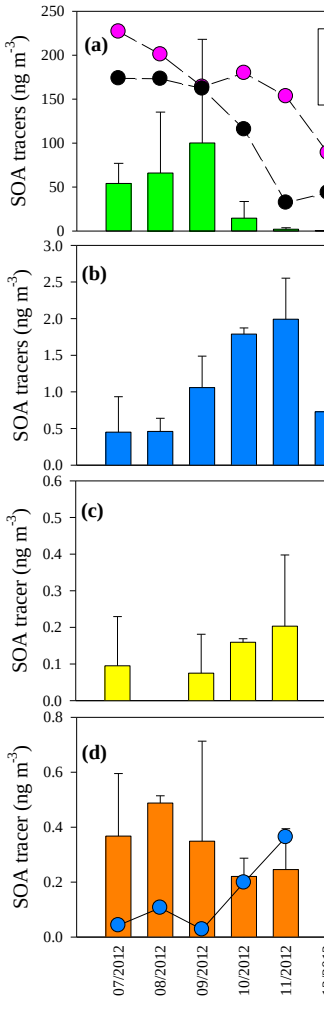

Deleted:

Formatted: Font: (Default) Times New Roman

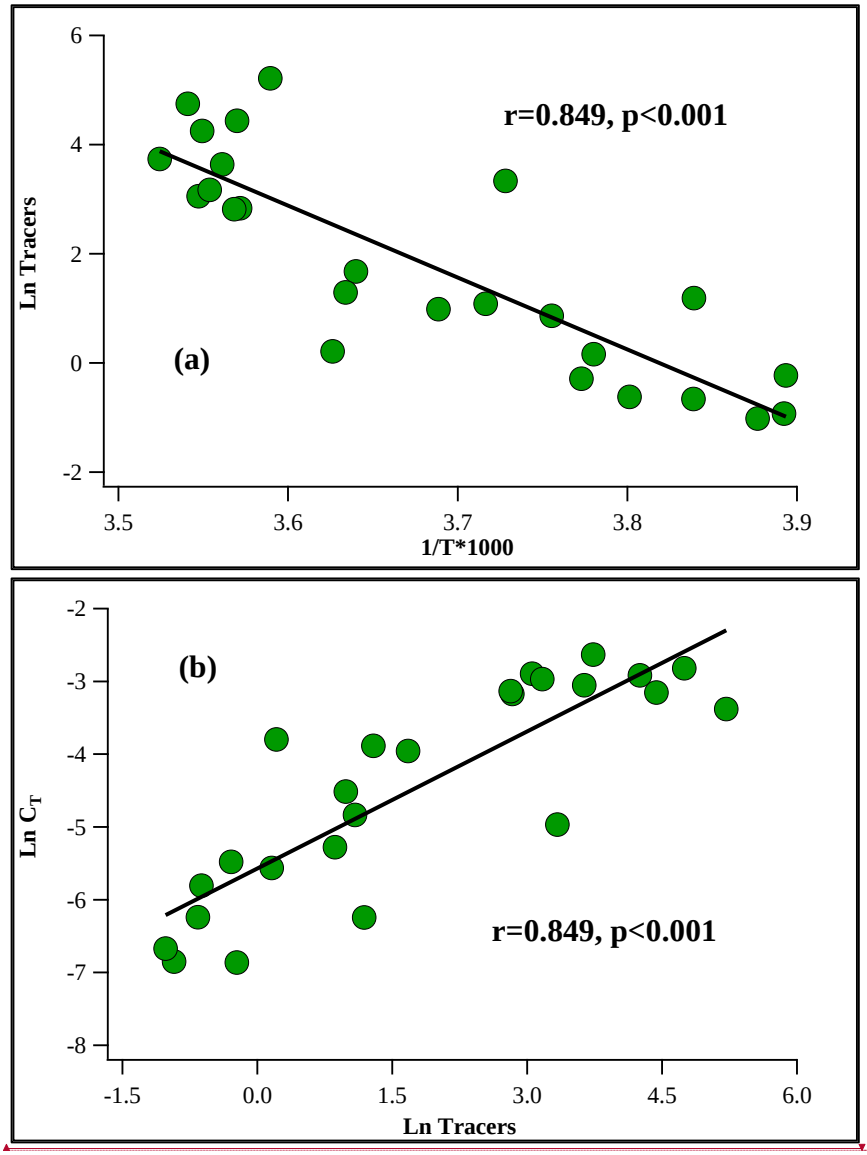

Figure 3 Correlations of SOA_I tracers with temperature (a) and C_T (b).

Formatted: Font: (Default) Times New Roman, 10 pt

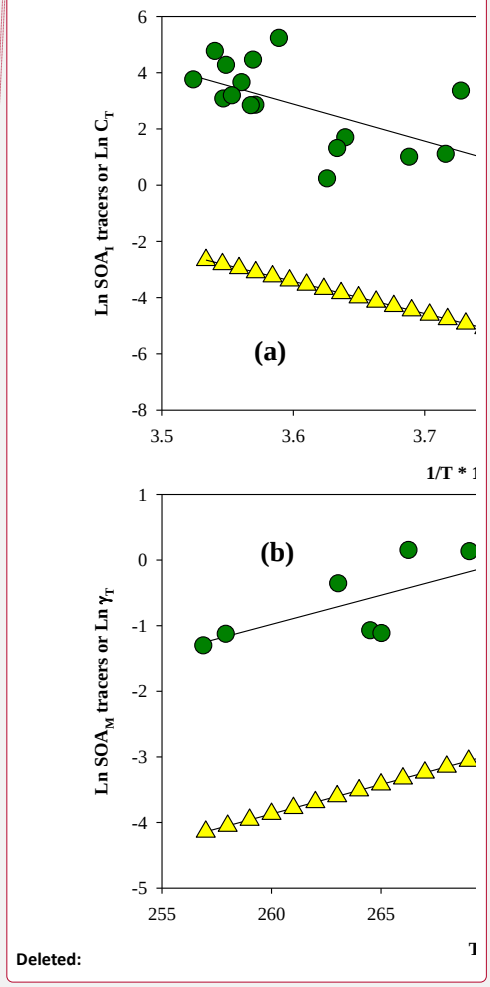

Deleted:

Deleted: Figure 3 Temperature dependences of SOA_I tracers in the whole year (a) and SOA_M tracers during the period 2 (b). All correlations are significant ($p<0.001$).

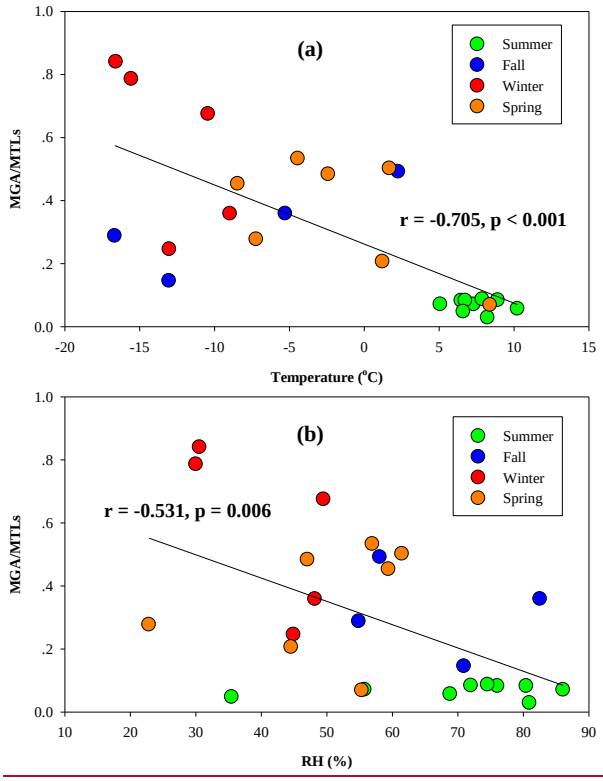

Figure 4 Correlations of MGA/MTL with temperature (a) and relative humidity (b). Summer is from July to September 2012 and from June to July 2013, fall is from October to November 2012, winter is from December 2012 to February 2013, and spring is from March to May 2013.

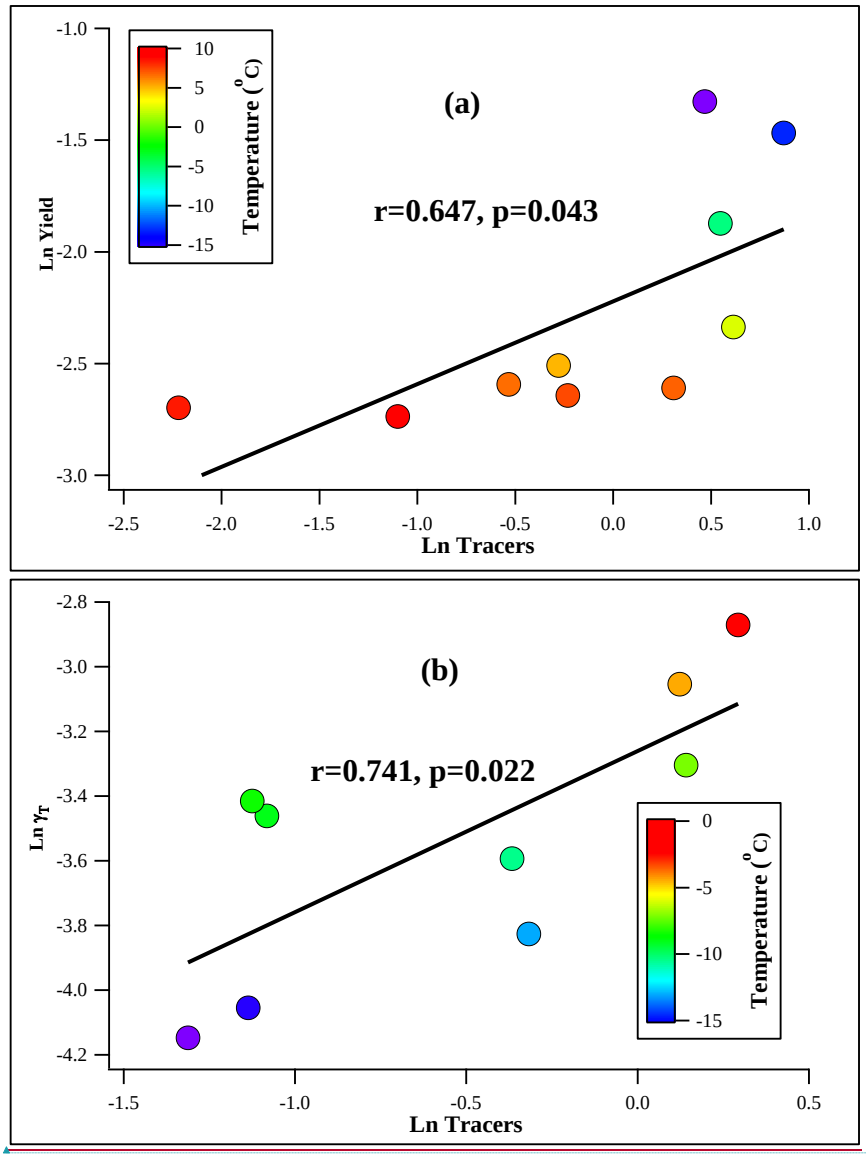

Figure 5 Correlation of SOA_M tracers with SOA yield in period 1 (a) and γ_T in period 2 (b)

Formatted: Font: (Default) Times New Roman, 小四

Formatted: Font color: Text 1

Formatted: Font: (Default) Times New Roman, Font color: Text 1

Formatted: Font: (Default) Times New Roman, Font color: Text 1

Formatted: Font: (Default) Times New Roman, Font color: Text 1

Formatted: Font color: Text 1

Formatted: Font color: Text 1

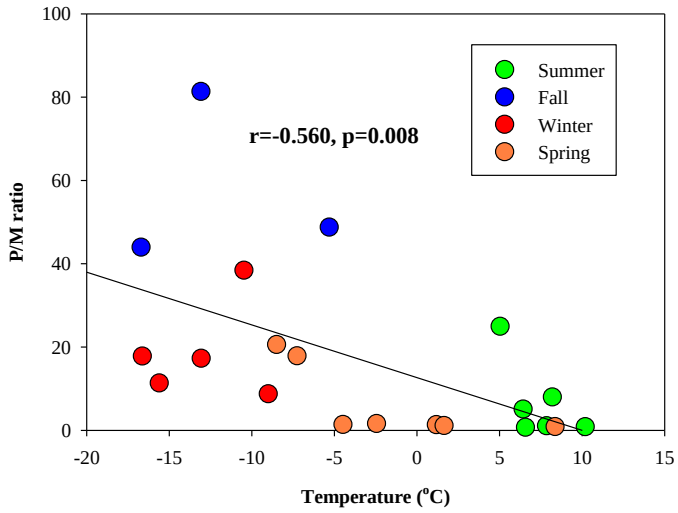

Figure 6 Negative correlation between P/M ratio and temperature

Formatted: Centered

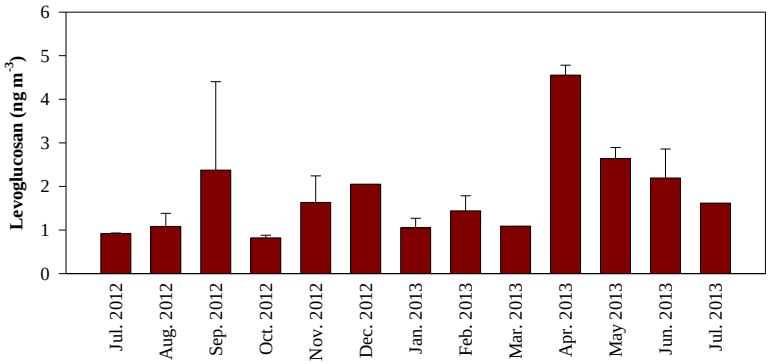

Figure 7 Monthly variation of biomass burning tracer, levoglucosan

Formatted: Font: (Default) Times New Roman

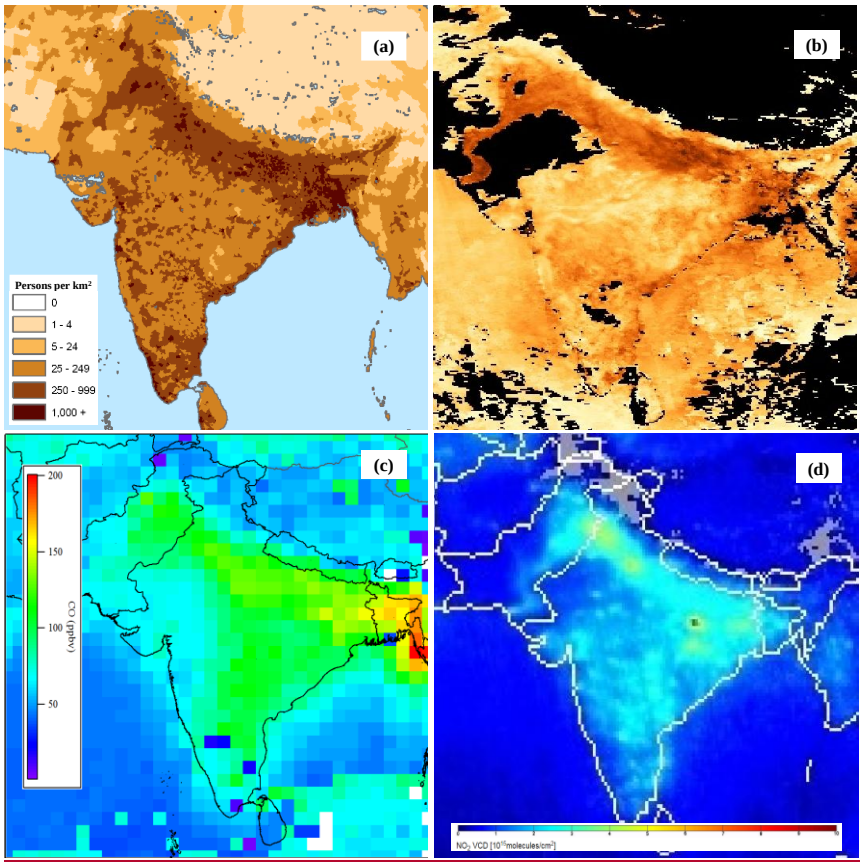

Figure 8 Spatial distribution of population density in 2000 (a), AOT (b), surface CO (c), and NO_2 VCD (d) in May 2013 over the Indian subcontinent and the TP.

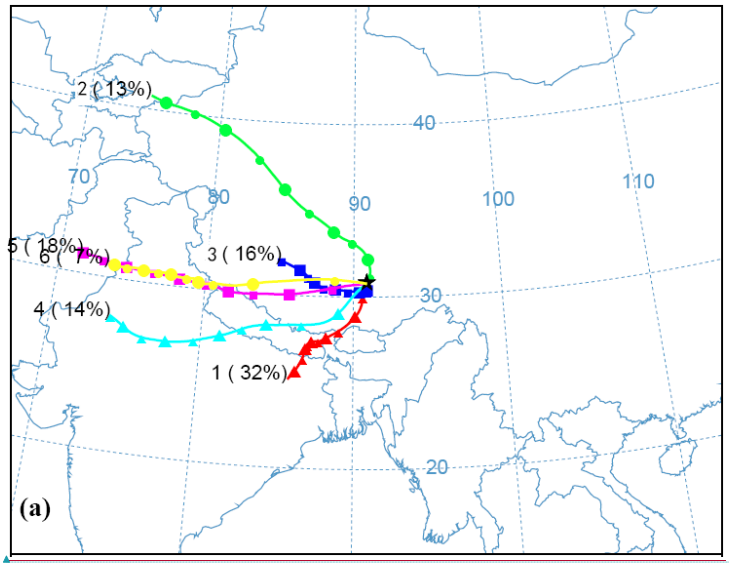

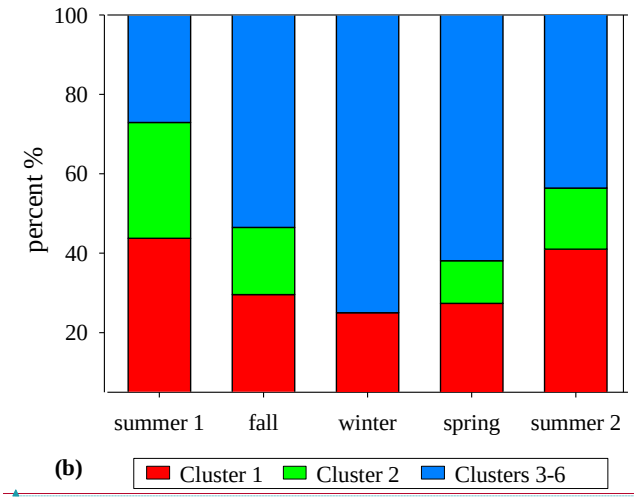

Figure 9 Cluster analyses of air masses at the NC site (a) and seasonal variations of clusters (b), based on 5-day backward trajectories during the sampling period. Summer 1 is from July to September 2012, fall is from October to November 2012, winter is from December 2012 to February 2013, spring is from March to May 2013, summer 2 is from June to July 2013.

Formatted: Font: (Default) Times New Roman

Formatted: Font: (Default) Times New Roman

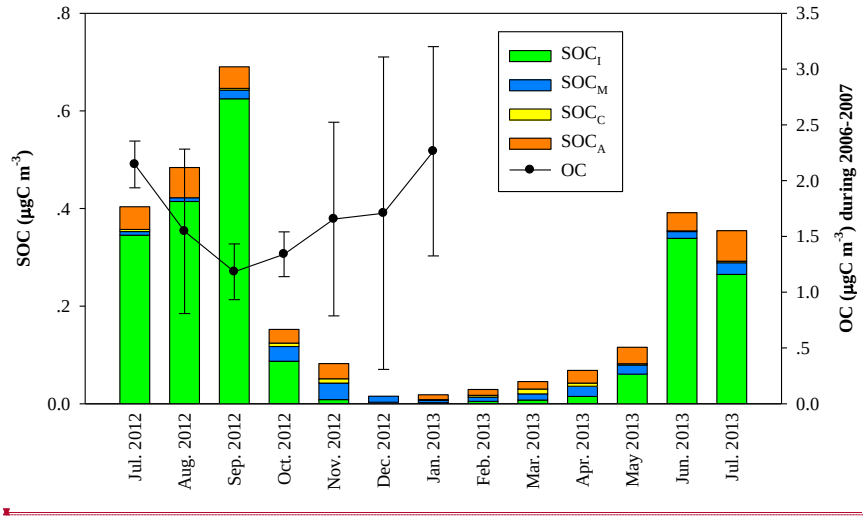

Figure 10 Seasonal variations of estimated SOC. OC data at the NC site during July 2006 to January 2007 were reported by Ming et al., (2010) and the err bar means one standard deviation in each month.

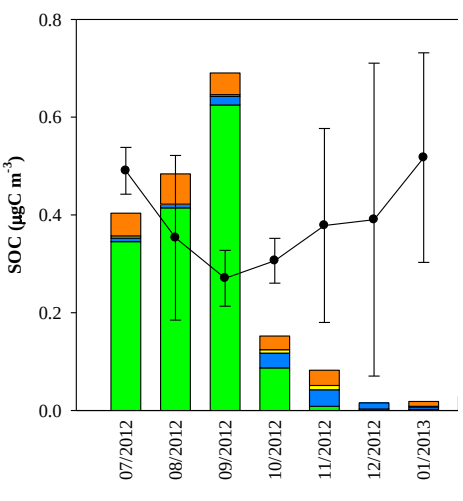

Deleted: .

Formatted: Font: (Default) Times New Roman

Deleted: 6

Table 1 SOA tracers at the NC site (ng m^{-3})

Month	Temp. ℃[a]	RH %[a]	SOA tracers				
			Isoprene	Monoterpenes	β-Caryophyllene	Aromatics	Sum
Jul. 2012	7.78	84	54.1 ±22.9[b]	0.45 ±0.48	0.10 ±0.13	0.37 ±0.23	55.0 ±22.5
Aug. 2012	7.70	76	66.0 ±69.3	0.46 ±0.18	nd[c]	0.49 ±0.03	67.0 ±69.1
Sep. 2012	5.92	66	100 ±118	1.06 ±0.43	0.08 ±0.11	0.35 ±0.36	102 ±118
Oct. 2012	-1.50	70	14.7 ±19.0	1.79 ±0.08	0.16 ±0.01	0.22 ±0.07	16.8 ±18.9
Nov. 2012	-14.9	63	2.04 ±1.76	1.99 ±0.56	0.20 ±0.19	0.25 ±0.15	4.48 ±2.66
Dec. 2012	-13.0	45	0.52	0.73	nd	nd	1.25
Jan. 2013	-16.1	30	0.38 ±0.02	0.30 ±0.04	0.03 ±0.01	0.08 ±0.01	0.78 ±0.01
Feb. 2013	-9.69	49	0.86 ±0.45	0.52 ±0.25	0.09 ±0.02	0.09 ±0.01	1.55 ±0.22
Mar. 2013	-7.83	41	1.56 ±1.15	0.74 ±0.59	0.23 ±0.25	0.12 ±0.17	2.65 ±2.15
Apr. 2013	-3.42	52	2.82 ±0.20	1.24 ±0.15	0.15 ±0.03	0.20 ±0.03	4.40 ±0.11
May 2013	3.77	54	10.1 ±9.70	1.11 ±0.13	0.06 ±0.06	0.27 ±0.19	11.5 ±9.97
Jun. 2013	7.25	55	54.1 ±42.9	0.83 ±0.18	0.03 ±0.04	0.30 ±0.02	55.3 ±42.8
Jul. 2013	10.2	69	41.9	1.41	0.07	0.49	43.9
Annual	-1.64	58	26.6 ±44.2	0.97 ±0.57	0.09 ±0.10	0.25 ±0.18	28.0 ±44.2

[a] Temperature and RH are monthly averages; [b] one standard deviation; [c] "nd" means not detected.

Formatted Table
Formatted: Superscript
Formatted: Superscript
Deleted: 07
Formatted: Superscript
Deleted: 08
Deleted: [b]
Deleted: 09
Deleted: 10
Deleted: 11
Deleted: 12
Deleted: 01
Deleted: 02
Deleted: 03
Deleted: 04
Deleted: 05
Deleted: 06
Deleted: 07
Formatted: Not Superscript/ Subscript
Formatted: Not Superscript/ Subscript
Deleted: [b]

Table 2 SOA tracers in remote places on the global range (ng m^{-3})

Locations		Seasons	References	SOA tracers			
				Isoprene [a]	**Monoterpenes** [a]	**β-Caryophyllene**	**Aromatics**
Tibetan Plateau	Nam Co Lake	Whole year	This study	26.6(0.36-184) [b]	0.97(0.11-2.39)	0.09(nd-0.40)	0.25(nd-0.61)
	Qianghai Lake	Summer	(Li *et al.* 2013)	2.50(0.13-7.15)	2.95(0.30-10.4)	0.87(0.05-2.41)	na [c]
	Himalayas	Summer-autumn	(Stone *et al.* 2012)	30.7(5.5-105)	13.2(5.6-31.3)	1.6(1.1-2.3)	na
Arctic	Alert	Winter-Summer	(Fu *et al.* 2009)	0.3(0.08-0.567)	1.6(0.138-5.3)	0.12(0.01-0.372)	na
	Arctic Ocean	Summer	(Fu *et al.* 2013)	4.0(0.16-31.8)	4.8(0.44-24.1)	0.017(0.005-0.048)	na
Global oceans	Low- to mid-latitude	Fall-Spring	(Fu *et al.* 2011)	3.6(0.11-22)	2.7(0.02-15)	0.32(0-2.5)	na
	Antarctic to Arctic	Summer	(Hu *et al.* 2013)	8.5(0.018-36)	3.0(0.05-20)	na	na
	North Pacific and Arctic	Summer	(Ding *et al.* 2013)	0.62(0.12-1.45)	0.06(0.01-0.25)	0.002(nd-0.03)	nd [d]

[a] compositions are different in different studies. [b] data range in brackets. [c] "na" means not available. [d] "nd" means not detected.

Formatted: Font: (Default) Times New Roman